On the Inverse Fractal Problem for Two Dimensional Disjoint Polyhulled Attractors

by

A. Deliu,[1] J. Geronimo,[2] and R. Shonkwiler[1]
School of Mathematics
Georgia Institute of Technology
Atlanta, GA 30332
e-mail: shenk@math.gatech.edu

1 Introduction

We use the term *fractal* in the sense of (Barnsley, 1988), as a set generated by an Iterated Function System (*IFS*). An iterated function system $\mathcal{W}$ is taken to be a finite set of contractive affine maps $w_i : X \to X$, $i = 1, 2, \ldots, N$, defined on a compact metric space X to itself. Associated with an *IFS* is a unique subset $A = A(\mathcal{W})$ of X, the *attractor* of $\mathcal{W}$, which is characterized by the *tiling property*, (Hutchinson, 1981),

$$A = \bigcup_{i=1}^{N} w_i(A). \tag{1.1}$$

The sets $w_i(A)$ are the *tiles* of A (relative to $\mathcal{W}$) and the maps w_i their *generators*. Letting C_A denote the convex hull of A, the *first level tiles* or *hull tiles* of A relative to $\mathcal{W}$ are the sets $w_i(C_A)$, $i = 1, \ldots, N$. The existence of A can be demonstrated by realizing it as the fixed point under the set map, $\mathbf{W}(B) = \cup_{i=1}^{N} w_i(B)$ which is a contraction in the space of non-empty compact subsets of X under the Hausdorff metric (Barnsley, 1988). Our principal interest here is with two dimensional attractors and consequently X will be taken as the unit square of $\mathbf{R}^2$. By appropriate scaling, an arbitrary two dimensional attractor can be realized as a subset of this square. Hence in what follows, each map w is of the form $w = W + \mathbf{b}$ where W is a 2×2 matrix and $\mathbf{b}$ is a 2 dimensional vector. The trivial constant map, $w\mathbf{x} = \mathbf{b}$ for all $\mathbf{x}$, can be used only to insert individual points at arbitrary places in the attractor. We will not consider such attractors. Similarly, we will not consider attractors resulting from iterated functions systems containing singular

[1] Partially Supported by N.S.F. Grant G–37–653
[2] Partially Supported by N.S.F. Grant

maps. Most, if not all, of our results continue to hold for non-constant singular maps but a great many new cases result from their consideration which we leave for the reader.

We also consider one dimensional attractors. An *IFS* of one dimensional maps, $\hat{w}(x) = sx + b$, may be embedded in the class of two dimensional iterated function systems in many ways, for example by setting

$$w(\mathbf{x}) = \begin{pmatrix} s & 0 \\ 0 & s \end{pmatrix} \begin{pmatrix} x \\ y \end{pmatrix} + \begin{pmatrix} b \\ b \end{pmatrix}.$$

The diagonal of the square of the resulting two dimensional attractor is a root two enlarged replica of the original one dimensional attractor.

Attractors may be graphically rendered to produce wonderfully detailed monochrome images on a computer screen or the printed page. The fractal shrub of fig. 7 is such an example. By adjusting the generating maps of an *IFS*, the resulting image may be controlled and can have an appearance ranging from classical geometric objects, to natural objects, to highly abstract objects with fractal dimension not equal to the topological dimension, (Mandelbrot, 1982). The *forward problem* of fractal geometry is that of rendering the attractor of a given *IFS*.

Conversely, the *inverse problem* of fractal geometry is that of determining the *IFS* maps which produce a given attractor. The problem has been previously studied, frequently in the more general context of invariant measures on fractals, by (Abenda and Turchetti, 1989), (Barnsley,Ervin,Hardin,Lancaster, 1985), (Cabrelli, Forte, Molter, Vrscay, 1992), (Cabrelli, Molter, Vrscay, 1992), (Diaconis and Shahshahani, 1986), (Handy and Mantica,to appear), (Mantica and Sloan, 1989), (Vrscay and Roehrig, 1989), (Vrscay, 1990), (Vrscay, 1991a), (Vrscay, 1991b), (Bessis and Demko, 1990), (Stricthartz, 1993). Most of these papers treat the one dimensional case using the theory of moments of measures. However, up to now the numerical implementation of the moment approach has proved impractical.

In this work we present an entirely different approach to solving the inverse problem, one that is geometrically based. Our methods can be applied to a reasonably large class of one and two dimensional attractors which moreover are important in image applications, the class of polyhulled disjoint attractors (PHD attractors). This class includes those shown in figures 14–16. We formally define them in section 2. (The method also applies to figures 10–13 as these are "essentially disjoint.") Given an attractor A of this class we show how to find a $\mathcal{W}$ so that $A = A(\mathcal{W})$ exactly. In section 2 we also introduce refinement *IFS*'s and the Extreme Points Theorem, the principal result on which our work is based. This leads to the notion of formative and decorative tiles.

Our method also makes use of the elementary properties of the orbits of points under affine contractions. The *orbit* of a point $\mathbf{x}$ under the map w is the sequence of iterates

$w^k(\mathbf{x})$, $k = 0, 1, \ldots$. In section 3 we detail the correspondence between the eigenvalues and eigenvectors of a formative map and geometrical features of its trajectories, a continuous version of an orbit. This leads to the notion of natural coordinate systems. In section 4 we express these salient features in terms of polar coordinates based at the extreme point under study.

A major obstacle in our approach to solving the inverse problem is that the orbits of all the points of an attractor are mixed together and must be disentangled. In section 5 we introduce a certain edge or margin tracking tool, the *springbar function*, for this purpose and for eliciting the geometrical properties of trajectories. In section 6 we introduce the *gap analysis* for recovering the multiplicative periodicity of an orbit which was lost in its trajectory and enabling the calculation of the eigenvalues associated with a trajectory.

Ultimately the main task is that of distinguishing among several cases classified by eigenvalues. As each tool is introduced, we detail its application to each spectral case.

In section 7 we show how to calculate the encoding of decorative tiles. Again our approach is based on spectral methods.

Actually our geometrical method works for attractors beyond the class of polyhulled disjoint ones, for example on attractors all of whose tiles have extreme points, such as the fractal shrub. Further, by adding limiting techniques, the subject of section 8, the class which may be inverted expands to include just touching (see §2) polyhulled attractors as well, such as the Dragon attractor, fig. 9. Moreover if only approximate solutions are required, the *Collage Theorem* of (Barnsley,Ervin,Hardin,Lancaster, 1985) which states, roughly, that *the better an image can be tiled by affine copies of itself, the closer will be the attractor of the resulting IFS to the image*, suggests that the class of solvable images can be greatly expanded although we have not investigated this.

A major unfinished extension of the work, which the authors believe is possible, is to non-polyhulled attractors such as the Black Spleenwort fern shown in fig. 8.

While the primary interest here is in the theoretical solution of the inverse problem, our geometrical method is amenable to numerical implementation. As has been previously noted, *IFS* encoding results in enormous data compression and hence significant commercial value, (Barnsley and Sloan, 1985).

Summary of the Method.

1. At each extreme point $\mathbf{p}$ of the convex hull C_A of A perform a Springbar Analysis to elicit sufficient parameter information enabling the calculation of trajectory maps at $\mathbf{p}$.
2. Using the trajectory maps, calculate the domain of invariance and supporting trajectories at each extreme point. Distinguish primary versus secondary extreme points.

3. With the trajectory maps at $\mathbf{p}$ in hand, for each $\mathbf{x}$ in the domain of invariance at $\mathbf{p}$, perform a gap analysis on the fractal dust corresponding to the trajectory through $\mathbf{x}$ to calculate its multiplicative period, $\lambda_{\mathbf{x}}$.
4. Using the collection of spectra $\lambda_{\mathbf{x}}$, calculate the minor eigenvalue and hence the locally formative map at $\mathbf{p}$. This solves primary maps; it remains to solve secondary maps.
5. By matching spectra, determine the primary pre-image for each secondary extreme point. By matching respective supporting trajectories calculate each secondary decorative map; it remains to calculate interior decorative maps.
6. By means of fat-curves, well order interior tiles. Using the same techniques as for secondary points above, successively solve, and "color", the interior tiles until the entire attractor is colored.

2 The Class of Disjoint Polyhulled Attractors

2.1 *Equivalence classes of IFS's*

It is well-known, and easy to show by example, that distinct iterated function systems can have identical attractors. (We do not regard a permutation of the maps of an *IFS* as constituting a distinct one.) For example if the attractor has symmetries, groups of transformations, invariant under the particular symmetry, can be used to construct equivalent systems.

Let $\mathcal{E}(A)$ denote the class of all iterated function systems whose attractor is A,

$$\mathcal{E}(A) = \{\mathcal{W} \ : \ A(\mathcal{W}) = A\}$$

or $\mathcal{E}(A) = \emptyset$ if A is not the attractor of any *IFS*.

Definition 1. We say an affine map w is *invariant* for the attractor A if $w(A) \subset A$.

Evidently any invariant map can be added to an *IFS* and the result will again be an *IFS* for the same attractor. Conversely, it may be possible to remove one or more maps from an *IFS* without affecting its attractor. We define the index of A to be the smallest number of maps which will generate the attractor A,

$$\text{index}(A) = \min\{\text{card}(\mathcal{W}) : \mathcal{W} \in \mathcal{E}(A)\}.$$

If $\mathcal{W} = \{w_1, \ldots, w_N\}$ is an *IFS* for A, then the compositions $w_1 \circ w_i(A)$, $i = 1, \ldots, N$, subtile $w_1(A)$. Hence

$$w_1\mathcal{W} = \{w_1 \circ w_1 \circ w_1^{-1}, w_1 \circ w_2 \circ w_1^{-1}, \ldots, w_1 \circ w_N \circ w_1^{-1}\}$$

is an *IFS* for $w_1(A)$.

More generally, let $\mathcal{W}$ and $\mathcal{W}'$ be two iterated function systems for an attractor A. We say $\mathcal{W}'$ is a *refinement* of $\mathcal{W}$ if every tile $w'(A)$ of $\mathcal{W}'$ is contained in some tile of $\mathcal{W}$, that is $w'(A) \subset w(A)$, for some $w \in \mathcal{W}$. Given iterated function systems $\mathcal{W}_1, \mathcal{W}_2 \in \mathcal{E}(A)$, with $N_k = \text{card}(\mathcal{W}_k)$, $k = 1, 2$, one of their *common refinements*, $\mathcal{W} = \mathcal{W}_1 \circ \mathcal{W}_2$, is the set of all compositions

$$\mathcal{W} = \{w_i^1 \circ w_j^2 \, : \, w_i^1 \in \mathcal{W}_1, w_j^2 \in \mathcal{W}_2\}.$$

Since $\mathcal{W}_2$ induces a tiling of A, it follows that $w_i^1 \circ w_j^2(A) \subset A$, $i = 1, \ldots, N_1$, $j = 1, \ldots, N_2$, and

$$\bigcup_{j=1}^{N_2} w_i^1 \circ w_j^2(A) = w_i^1(\bigcup_{j=1}^{N_2} w_j^2(A)) = w_i^1(A). \tag{2.1}$$

Hence

$$\bigcup_{i=1}^{N_1} \bigcup_{j=1}^{N_2} w_i^1 \circ w_j^2(A) = A$$

showing that $\mathcal{W} \in \mathcal{E}(A)$. Of course the same holds for their other common refinement $\mathcal{W}_2 \circ \mathcal{W}_1$. This proves the following.

Proposition 1. *Let $\mathcal{W}_1, \mathcal{W}_2 \in \mathcal{E}(A)$, then also the refinement $\mathcal{W}_1 \circ \mathcal{W}_2 \in \mathcal{E}(A)$.*

Equation (2.1) also shows that each tile $w_i^1(A)$ of $\mathcal{W}_1$ is itself *subtiled* by the $\mathcal{W}_2$ tiles $w_i^1 \circ w_j^2(A)$, in a manner similar to the tiling of A by $\mathcal{W}_2$. Thus each tile of the common refinement $\mathcal{W}$ is either disjoint from or wholly contained in each tile of its second argument $\mathcal{W}_1$.

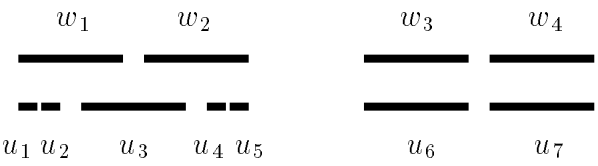

fig. 1, First level tiles of the Partial Refinement Example

Remark. *It is possible for two iterated function systems having the same attractor, that the tiles of one only partially refine tiles of the other. This occurs for the 1-D attractor due to the following two iterated function systems, see fig. 1,* [1]

[1] *This example is due to George Donovan.*

$$\mathcal{W} = \{w_1(x) = \frac{2}{11}x, \quad w_2(x) = \frac{2}{11}x + \frac{12}{55},$$
$$w_3(x) = \frac{2}{11}x + \frac{3}{5}, \quad w_4(x) = \frac{2}{11}x + \frac{9}{11}\}$$

and

$$\mathcal{U} = \{u_1(x) = \frac{4}{121}x, \quad u_2(x) = \frac{4}{121}x + \frac{24}{605}, \quad u_3(x) = \frac{2}{11}x + \frac{6}{55},$$
$$u_4(x) = \frac{4}{121}x + \frac{18}{55}, \quad u_5(x) = \frac{4}{121}x + \frac{222}{605}, \quad u_6 = w_3, \quad u_7 = w_4\}.$$

Obviously a common refinement may be further subtiled by yet another equivalent *IFS* for its attractor. In particular we may take $\mathcal{W}_2$ above to be $\mathcal{W}_1$ in which case we write

$$\mathcal{W}_1^2 = \mathcal{W}_1 \circ \mathcal{W}_1.$$

More generally, the *power refinements* of $\mathcal{W}$ are, for some k,

$$\mathcal{W}^k = \mathcal{W} \circ \ldots \circ \mathcal{W}, \qquad k \text{ times}$$
$$= \{w_{i_1} \circ w_{i_2} \circ \ldots \circ w_{i_k} \ : \ w_{i_j} \in \mathcal{W}, j = 1, \ldots, k\}.$$

2.2 *Disjoint Attractors*

Definition 1. An *IFS* $\mathcal{W}$ is *disjoint* if its tiles are pairwise disjoint, $w_i(A) \cap w_j(A) = \emptyset$, for $1 \leq i < j \leq N$. An attractor A is *disjoint* if it has at least one disjoint *IFS*, that is $\mathcal{W}$ is disjoint for some $\mathcal{W} \in \mathcal{E}(A)$.

The following is an elementary observation stemming from the compactness of tiles.

Proposition 1. *Given a disjoint IFS $\mathcal{W}$ for A, there exist $\delta > 0$ such that*

$$dist(w_i(A), w_j(A)) \geq \delta \qquad \text{for all } w_i, w_j \in \mathcal{W},\ i \neq j.$$

Corollary 1. *Let A be a disjoint attractor and $w_1(A)$ and $w_2(A)$ be two distinct tiles for some disjoint $\mathcal{W} \in \mathcal{E}(A)$. Let $\mathbf{x}(t)$, $a \leq t \leq b$, be a curve in $\mathbf{R}^2$ such that $\mathbf{x}(a) \in w_1(A)$ and $\mathbf{x}(b) \in w_2(A)$. Then for some interval $t \in (c, d)$, $\mathbf{x}(t) \cap A = \emptyset$.*

Proposition 2. *Let $\mathcal{W}_1$ and $\mathcal{W}_2$ be disjoint IFS's for A, then their common refinements are also disjoint.*

Proof. Let $\mathcal{W}_k = \{w_1^k, w_2^k, \ldots\}$, $k = 1, 2$. By symmetry it suffices to consider $\mathcal{W}_1 \circ \mathcal{W}_2$. If $i \neq j$ then $w_i^k(S) \cap w_j^k(S) = \emptyset$, $k = 1, 2$, for any $S \subset A$. Hence if either $i \neq k$ or $j \neq m$ then

$$w_i^1 \circ w_j^2(A) \cap w_k^1 \circ w_m^2(A) = \emptyset.$$

∎

Definition 2. An attractor A is said to be *just touching* if it has an *IFS* $\mathcal{W}$ satisfying the open set condition and $w_i(A) \cap w_j(A) \neq \emptyset$ for some generators $w_i \neq w_j$. The *open set condition* holds for $\mathcal{W}$ if there exists a non-empty open set $\mathcal{O}$ such that $w_i(\mathcal{O}) \cap w_j(\mathcal{O}) = \emptyset$, for all $i \neq j$, and $\cup_i w_i(\mathcal{O}) \subset \mathcal{O}$, cf. (Hutchinson, 1981).

2.3 *The Convex Hull and its Extreme Points*

Given a line ℓ in the plane, $\ell = \{(x, y) : ax + by = c\}$, where $a, b, c \in \mathbf{R}$, let $J_\ell = \{(x, y) : ax + by \geq c\}$ be the closed half space consisting of ℓ itself and its open "positive" half space. We say ℓ *supports* a set S if $S \subset J_\ell$ and $S \cap \ell \neq \emptyset$. We say $\mathbf{p} \in S$ is an *extreme point* of S if $\mathbf{p}$ belongs to at least two distinct supporting lines of S. Let ext(S) denote the set of extreme points of S.

Let A be an attractor, its *convex hull*, C_A, is the intersection of all closed half-spaces containing A,

$$C_A = \bigcap_{\ell \in L} J_\ell,$$

where $\ell \in L$ if and only if $A \subset J_\ell$. Evidently C_A is closed and is the smallest convex set which contains A. We orient the boundary of the convex hull as usual, counterclockwise. If A is the attractor of an *IFS*, then A is compact and thus C_A is a compact convex set.

Definition 1. An *IFS* is *strongly disjoint* if $w_i(C_A) \cap w_j(C_A) = \emptyset$ for all $i \neq j$ where C_A is the convex hull of A. Likewise, an attractor A is *strongly disjoint* if it has a strongly disjoint *IFS*. Fig. 14 shows a disjoint not strongly disjoint gaskettype attractor.

It is obvious that Proposition 2.2.2 continues to hold for strongly disjoint attractors.

Definition 2. An affine map w is *invertible* for an attractor A if it is invariant for A and for every $\mathbf{x} \in w(C_A) \cap A$, $w^{-1}(\mathbf{x}) \in A$. An *IFS* is *invertible* if every one of its maps is.

Theorem 1. *If $\mathcal{W}$ is a strongly disjoint IFS for A, then $\mathcal{W}$ is invertible.*

Proof. Since $w(C_A) \supset w(A)$, this follows easily from (1.1). ∎

Theorem 2. *If $\mathcal{W}$ is a disjoint IFS for A and $w \in \mathcal{W}$, then w^k is invertible for A for some $k = 1, 2, \ldots$.*

Proof. Since the $w_i(A)$, $w_i \in \mathcal{W}$, are disjoint compact sets, there is a $\delta > 0$ such that the set distance between every (distinct) pair of sets $w_i(A)$ and $w_j(A)$, $w_i, w_j \in \mathcal{W}$, exceeds δ. Now let k be sufficiently large that $\mathrm{diam}(w^k(A)) < \delta$. Then by (1.1), if $\mathbf{x} \in w^k(C_A) \cap A$, it follows that $\mathbf{x}$ can not lie in $w_i(A)$ for $w_i \neq w$. Hence $\mathbf{x} \in w(A)$ and so $w^{-1}(\mathbf{x}) \in A$. ∎

Corollary 1. *With k as in the Theorem, if $\mathbf{x} \in w^{k+n}(C_A) \cap A$, $n \geq 0$, then $w^{-i}(\mathbf{x}) \in A$ for $1 \leq i \leq n$. If G is an open subset of $w^k(C_A)$ disjoint from A, i.e. a gap in A, then $w^{k+n}(G)$ is a gap in A for all $n \geq 0$.*

Definition 3. An attractor A is *flat* if for some line ℓ, $A \subset \ell$. Obviously a flat attractor has exactly two extreme points and its convex hull consists of a line segment.

The following result, due to Berger is central to our work.

Theorem 3. *(Extreme Points.) Let A be the attractor of an iterated function system $\mathcal{W}$. Then every extreme point $\mathbf{p}$ of A is the image of an extreme point $\mathbf{q}$ of A under some generating map, that is*

$$ext(A) \subset \bigcup_{i=1}^{N} w_i(ext(A)).$$

Proof. (Berger, 1991).

The theorem allows, and it often occurs, that an extreme point $\mathbf{p}$ is the image of itself under a generating map. This is a sufficiently important case to warrant a definition.

Definition 4. An invariant map w for A is *formative* if its fixed point is also an extreme point of A, otherwise it is *decorative*. An extreme point $\mathbf{p}$ is a *primary* point or an *extreme fixed point* if it is the fixed point of some formative map, otherwise it is *secondary*.

Remark. *A single tile can have more than one extreme point, even if one of these is an extreme fixed point, cf. Gasketflip fig. 13, It is also possible that no extreme point is primary for a given IFS, cf. Dragontails fig. 10; however we will show below that there always exists an equivalent IFS for every polyhulled disjoint attractor in which at least one extreme point is primary and moreover in which every secondary extreme point is the image of some primary one.*

Proposition 1. *Let $\mathcal{W}_1, \mathcal{W}_2 \in \mathcal{E}(A)$ and suppose the extreme point $\mathbf{p}$ is the image of the extreme fixed point $\mathbf{q}$ under generating maps for both $\mathcal{W}_1$ and $\mathcal{W}_2$. Then relative to their common refinement $\mathcal{W}_1 \circ \mathcal{W}_2$, $\mathbf{q}$ remains primary and $\mathbf{p}$ is its image under some generating map.*

Proof. If $w^1(\mathbf{q}) = w^2(\mathbf{q}) = \mathbf{q}$ then also $w^1(w^2(\mathbf{q})) = \mathbf{q}$. Similarly, if $\hat{w}^1(\mathbf{q}) = \mathbf{p}$, then $\hat{w}^1(w^2(\mathbf{q})) = \mathbf{p}$. ∎

2.4 *The Class of Disjoint Polyhulled Attractors.*

Definition 1. An attractor is *polyhulled* if it has only finitely many extreme points. Figures 7–16, except fig. 8, are polyhulled.

Remark. *Every flat attractor is polyhulled.*

Theorem 2. *(Refinement.) Let A be a polyhulled attractor. Then there exists $\mathcal{W} \in \mathcal{E}(A)$ such that every extreme point $\mathbf{p}$ is the image $\mathbf{p} = w(\mathbf{q})$ of a primary point $\mathbf{q}$ of A under some generating map w. If in addition A is disjoint, then $\mathcal{W}$ can be chosen disjoint also.*

Proof. Let $\mathcal{W}$ be an *IFS* for A, if A is disjoint, take $\mathcal{W}$ to be disjoint also. Let $\mathbf{p}_0 = \mathbf{p} \in \text{ext}(A)$. By repeated application of the Extreme Points Theorem, there exists a sequence of extreme points $\mathbf{p}_1, \mathbf{p}_2, \ldots$, and maps $w_1, w_2, \ldots$ in $\mathcal{W}$ such that

$$\mathbf{p}_{i-1} = w_i(\mathbf{p}_i), \qquad i = 1, 2, \ldots .$$

But since there are at most finitely many distinct extreme points for polyhulled attractors, the sequence must cycle, i.e., for some non-negative integers j_0 and $k_{\mathbf{p}}$,

$$\mathbf{p}_j = \mathbf{p}_{j+k_{\mathbf{p}}}, \qquad j \geq j_0 .$$

If $k_{\mathbf{p}} = 0$, then $\mathbf{p}_{j_0}$ is the fixed-point of w_{j_0}. If $k_{\mathbf{p}} \neq 0$, consider the composition f

$$f = w_{j_0+1} \circ \ldots \circ w_{j_0+k_{\mathbf{p}}} .$$

Clearly $\mathbf{p}_{j_0}$ is the fixed-point of f. If $j_0 > 0$ then $\mathbf{p}$ itself is not a fixed-point. Instead it is the image

$$\mathbf{p} = w_1 \circ \ldots \circ w_{j_0}(\mathbf{p}_{j_0}).$$

of the extreme fixed point $\mathbf{p}_{j_0}$ under the composition $w = w_1 \circ \ldots \circ w_{j_0}$. Let $k = \max\{k_p, j_0\}$. Then the conclusion holds for this point $\mathbf{p}$ for the refinement $\mathcal{W}^k$ of $\mathcal{W}$.

By Proposition 2.3.1 above, if $\mathbf{r}$ is the image of an extreme fixed point of a generating map in $\mathcal{W}$, then it continues to be for $\mathcal{W}^k$ as well. Hence we may continue as above for each extreme point and arrive at a new *IFS* $\mathcal{W}' \supset \mathcal{W}$ satisfying the requirements of the conclusion. If the original *IFS* is disjoint, $\mathcal{W}'$ will be also. ∎

Corollary 1. *Every polyhulled attractor has at least one primary point for some IFS.*

Proof. From the proof of the Refinement Theorem, $\mathbf{p}_{j_0}$ is primary as is every extreme point in the cycle in the refined *IFS*. ∎

Remark. *In view of this result, the Dragontails attractor of fig. 10, has an IFS for which the 3 extreme points (0,0), (1,0), and (0,1) are primary; in fact the cubic refinement $\mathcal{W}^3$ contains the map*

$$w_1^3(\mathbf{x}) = \begin{pmatrix} \frac{1}{8} & 0 \\ 0 & \frac{1}{8} \end{pmatrix}$$

for which $(0,0)$ *is fixed.*

Definition 2. An affine contraction u is *locally invariant* for an attractor A if there exists a neighborhood $\mathcal{N}$ of its fixed point $\mathbf{p}$ such that $u(\mathcal{N} \cap A) \subset \mathcal{N} \cap A$ (u is not necessarily part of an *IFS* for A). A locally invariant map whose fixed point is also an extreme point of A is *locally formative*. An extreme point $\mathbf{p}$ of A is *locally primary* if it is the fixed point of some locally invariant map for A.

Theorem 3. *Every extreme point of a polyhulled disjoint attractor is locally primary.*

Proof. Let $\mathbf{p}$ be such an extreme point. By the construction of the Refinement Theorem, there is a non-singular affine map w such that $\mathbf{p} = w(\mathbf{q})$ where $\mathbf{q}$ is primary. Let f be an affine map showing $\mathbf{q}$ is primary, then $h = wfw^{-1}$ is the required locally invariant map. For if W and F are the linear parts of w and f respectively, $w = W + (\mathbf{p} - W\mathbf{q})$ and $f = F + (\mathbf{q} - F\mathbf{q})$, then $h = WFW^{-1} + (\mathbf{p} - WFW^{-1}\mathbf{p})$. Clearly h has the required properties on any open set containing the w tile of $\mathbf{p}$ and disjoint from all other tiles. ∎

3 Orbits of 2-D Affine Maps

From Theorem 2.4.3 every extreme point $\mathbf{p}$ of an attractor A is the fixed point of some locally formative map f. In this section we draw a correspondence between the eigenvalues and eigenvectors of such a map and the structure of A near $\mathbf{p}$. Letting L be the corresponding Jordan form matrix and S the matrix whose columns are the eigenvectors, then the linear part F of f is given by

$$F = SLS^{-1}. \tag{3.1}$$

The translational part of f is then easily determined knowing its fixed point $\mathbf{p}$, see equation (3.2). Thus a complete list of characterizing information for an affine map consists of (a) its eigenvalues, (b) its eigenvectors, and (c) its fixed point.

Since the eigenvalues of real 2×2 matrices are either both real or are complex conjugates, we may divide the study into four cases: (E_1) the eigenvalues are real and distinct, (E_2) the eigenvalues are equal (hence real) and there are two linearly independent eigenvectors, (E_3) the eigenvalues are equal and there is only one linearly independent eigenvector, and (E_4) the eigenvalues are complex. As noted in the Introduction, we exclude from consideration here attractors resulting from iterated function systems containing singular maps. A disjoint tile resulting from such a map will be confined to a line segment. Our methods can handle such attractors, but their consideration results in having to deal with many additional special cases which we leave for the reader.

By our definition of extreme point, if the fixed point of a transformation lies on at most one supporting line then it cannot at the same time be an extreme point of the

attractor. One of the aims of this section is to characterize, in terms of spectral properties, those maps which can have extreme fixed-points and those which cannot.

3.1 *Translation Simplification*

The general form of a 2-D affine transformation f is

$$\begin{pmatrix} r \\ s \end{pmatrix} = \begin{pmatrix} a & b \\ c & d \end{pmatrix} \begin{pmatrix} x \\ y \end{pmatrix} + \begin{pmatrix} e \\ f \end{pmatrix} = F\mathbf{x} + \mathbf{b}$$

or $\mathbf{r} = f\mathbf{x}$. Here F is the linear part of f and $\mathbf{b}$ is the translation. All affine maps f in this work are assumed to be contractive (and hence uniformly contractive),

$$\|f\mathbf{x} - f\mathbf{y}\| \le s\|\mathbf{x} - \mathbf{y}\| \qquad \text{for some} \quad 0 < s < 1.$$

By the uniform contraction property, every orbit tends as a geometric series to a unique limit $\mathbf{p}$; thus for every $\mathbf{x}$,

$$\lim_{n\to\infty} f^n\mathbf{x} = \mathbf{p}.$$

Such a limit point $\mathbf{p}$ is by necessity the unique fixed point of f,

$$f\mathbf{p} = \mathbf{p}.$$

In terms of F the fixed point satisfies the equation

$$F\mathbf{p} + \mathbf{b} = \mathbf{p} \qquad \text{or} \qquad (I - F)\mathbf{p} = \mathbf{b} \tag{3.2}$$

from which $\mathbf{p}$ can be found since $I - F$ is not singular when F is a contraction. On the other hand, in solving the encoding problem, this equation can be used in the converse way to calculate $\mathbf{b} = \left(\begin{smallmatrix} e \\ f \end{smallmatrix}\right)$ knowing F and $\mathbf{p}$.

Now translate the origin to the fixed point $\mathbf{p}$. Let $\mathbf{x}' = \mathbf{x} - \mathbf{p}$, and also $\mathbf{y}' = \mathbf{y} - \mathbf{p}$. Then

$$\mathbf{y}' = F\mathbf{x} + \mathbf{b} - \mathbf{p} = F\mathbf{x} + \mathbf{b} - (F\mathbf{p} + \mathbf{b}) = F(\mathbf{x} - \mathbf{p}) = F\mathbf{x}'.$$

Therefore by so translating, the study of orbits of affine maps is reduced to studying orbits of linear maps; in particular the problem is reduced from 6 parameters to 4, namely a, b, c, d.

In the sequel we assume the translation has been done and dispense with the use of primes to designate translated points. Thus $F\mathbf{x}$ and $f\mathbf{x}$ will be the same.

3.2 *Orbits in the Complex Case*

The next result shows that an affine map with complex eigenvalues cannot give rise to a primary point. As a result, we may exclude case (E_4) from further consideration in this section.

Theorem 1. *Let* $\mathbf{p}$ *be the fixed-point of an affine contraction with linear part* F *and let* Ω *be the orbit of* $\mathbf{x} \neq \mathbf{p}$. *If the eigenvalues of* F *are complex, then for every half-space* H *containing* $\mathbf{p}$, *both* H *and its complement* H' *meet* Ω. *Hence such a map cannot have an extreme fixed-point.*

Proof. Let F be the 2×2 real matrix with complex eigenvalues. For $0 \leq \theta \leq \pi$ define $\Delta(\theta)$ as follows. Let $\mathbf{u}$ be the unit vector at angle θ (from some fixed reference ray through $\mathbf{p}$), that is $\arg(\mathbf{u}) = \theta$, and let $\mathbf{v}$ be the unit vector $F\mathbf{u}/\|F\mathbf{u}\|$. Note that $\mathbf{v} \neq 0$ since 0 is not an eigenvalue of F. Put $\Delta(\theta) = \arg(\mathbf{v}) - \theta$ where $\arg(\mathbf{v})$ is the angle of $\mathbf{v}$ from the reference ray between $-\pi$ and π. Note that $\Delta(\theta) \neq 0$, $0 \leq \theta \leq \pi$, and $\Delta(\theta) \neq \pi$ for otherwise F would have a real eigenvector.

Assume $\Delta(0) > 0$ the other case being similar. Since $\Delta(\cdot)$ is continuous, and $\Delta(\pi) = \Delta(0)$, its graph is a connected compact subset of the rectangle $[0, \pi] \times [0, \pi]$. Let $m = \min \Delta(\theta)$ and $M = \max \Delta(\theta)$, $0 \leq \theta \leq \pi$. Then $0 < m \leq M < \pi$. That is m is the minimum angle by which F rotates a vector and M is the maximum angle. Now let H be a closed half-space whose boundary, ∂H, contains $\mathbf{p}$ and assume $\mathbf{x} \in H$, $\mathbf{x} \neq 0$, the case $\mathbf{x} \in H'$, the complement of H, being similar. We show $F^n\mathbf{x}$ must lie in H' for some n. Taking one of the rays of ∂H from $\mathbf{p}$ as a reference, let $\{\mathbf{x}, F\mathbf{x}, \ldots, F^k\mathbf{x}\}$ be the initial segment of the orbit of $\mathbf{x}$ whose arguments increase. Since $\Delta(\theta)$ is bounded below, this segment must be finite as shown. But then $\arg(F^{k+1}\mathbf{x}) \leq \arg(F^k\mathbf{x}) + M < \arg(F^k\mathbf{x}) + \pi$. Hence $F^{k+1}\mathbf{x} \in H'$. ∎

Corollary 1. *No map for a flat attractor can have complex eigenvalues.*

The orbits for the complex case spiral in toward the fixed point and conversely, if the orbits spiral, then the eigenvalues are complex, cf. the Dragon attractor fig. 9.

A linear map F may be decomposed into polar form $F = UR$ where U is unitary and R is symmetric, (Nagy, 1970). Suppose U is a rotation,

$$U = \begin{pmatrix} \cos\theta & -\sin\theta \\ \sin\theta & \cos\theta \end{pmatrix}, \qquad R = \begin{pmatrix} a & b \\ b & c \end{pmatrix},$$

then in some sense the symmetric part, R, attempts to rotate vectors not lying on an eigenmanifold toward its major eigenmanifold in spite of U. Orbits will not be spirals if θ is not too big.

Theorem 2. *Let* $F = UR$ *be the polar decomposition of the linear part of the affine contraction* f *and suppose* U *is a rotation. Let* R *have eigenvalues* ν_1 *and* ν_2 *respectively. Then* f *has spiral orbits if and only if*

$$\left(\frac{\nu_1 + \nu_2}{2}\right)^2 \cos^2\theta < \nu_1\nu_2 .$$

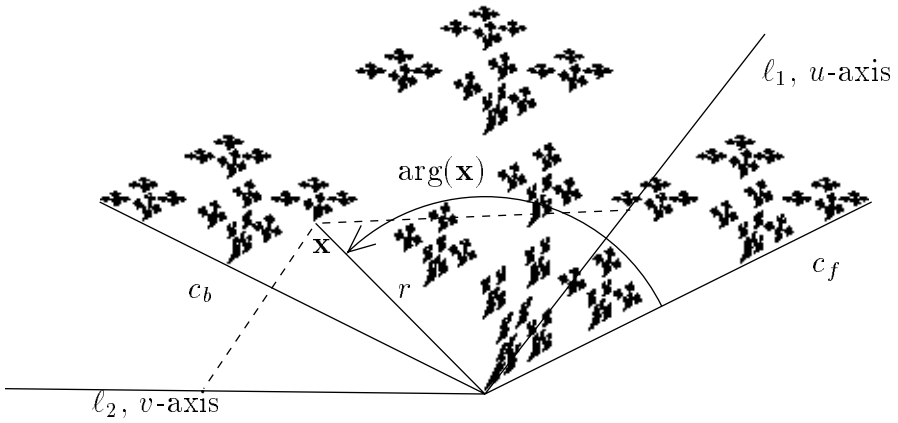

fig. 2, Natural and Polar Coordinates

Proof. Let S be the matrix of normalized eigenvectors of R, then S is a rotation matrix and hence $SUS^{-1} = U$. Thus the change of basis matrix $SFS^{-1} = SUS^{-1}SRS^{-1}$ and is

$$U \begin{pmatrix} \nu_1 & 0 \\ 0 & \nu_2 \end{pmatrix} = \begin{pmatrix} \nu_1 \cos\theta & -\nu_2 \sin\theta \\ \nu_1 \sin\theta & \nu_2 \cos\theta \end{pmatrix}.$$

Hence the characteristic polynomial of F is

$$\lambda^2 - ((\nu_1 + \nu_2)\cos\theta)\lambda + \nu_1\nu_2 .$$

It follows that the roots are complex if and only if the condition holds. ∎

Corollary 2. *For a rotational similitude, $\nu_1 = \nu_2$, the condition holds whenever $\theta \neq k\pi$, k an integer.*

Corollary 3. *A rotational similitude has at most one supporting line at its fixed point.*

Proof. A rotational similitude whose rotation angle is not equal to π, has complex eigenvalues and in this case the result follows from the theorem. On the other hand, clearly a 180^0 rotational contraction cannot have more than one supporting line at its fixed point. ∎

3.3 *Natural Coordinates*

Let $\mathbf{p}$ be an extreme point, let c_f be the ray coincident with the forward (counterclockwise) boundary or limb of the convex hull at $\mathbf{p}$ and c_b the ray coincident with the backward limb.

We define a local polar coordinate system, (r, θ), at $\mathbf{p}$ with r equal to the Euclidean distance of a point $\mathbf{x}$ from $\mathbf{p}$ and $\theta = \arg(\mathbf{x})$ measuring the angle counterclockwise from c_f, see fig. 2. In this subsection we define a coordinate system at $\mathbf{p}$ by defining unit coordinate vectors $\mathbf{e}_1$ and $\mathbf{e}_2$ whose definitions depend on the case E_1 – E_3.

Let λ_1 and λ_2 be the two real eigenvalues of a locally formative map F (having eliminated case E_4). Since F is a contraction, $|\lambda_1| < 1$, and $|\lambda_2| < 1$. In case E_1, we may assume without loss of generality that $|\lambda_1| \geq |\lambda_2|$. By the *major* eigenvalue, λ_1, we mean the larger in magnitude or, if their magnitudes are equal, the positive one. We refer to λ_2 as the *minor* eigenvalue. Let $\mathbf{e}_1$ and $\mathbf{e}_2$ be normalized eigenvectors corresponding to λ_1 and λ_2 respectively. Since $-\mathbf{e}$ is also an eigenvector if $\mathbf{e}$ is, they are determined only up to direction at this point. We will show in the sequel that exactly one ray of the eigenmanifold for λ_1 lies in the exterior of C_A; we take $\mathbf{e}_1$ to lie along the other ray, i.e. to point into the convex hull. In defining $\mathbf{e}_2$ we allow its direction to depend upon the context in such a way that when a point $\mathbf{x} \in A$ is chosen for some purpose, select the direction of $\mathbf{e}_2$ so that $\mathbf{x}$ has non-negative component along $\mathbf{e}_2$.

In case E_2 the locally formative map is given as $F = \lambda I$ where λ is the common eigenvalue and I is the identity map; that is F is a non-rotational similitude and every non-zero vector is an eigenvector. In this case we take the normalized vectors $\mathbf{e}_1$ and $\mathbf{e}_2$ to lie along c_f and c_b, the limbs of the convex hull, respectively.

In case E_3, the *geometrical multiplicity one* (or GM-1) case, we will show, as noted above, that the eigenmanifold has exactly one ray lying in the exterior of C_A; and as above, let the normalized eigenvector $\mathbf{e}_1$ lie along the opposite ray. Let $\mathbf{e}_2$ be perpendicular to $\mathbf{e}_1$ of unit length. Let its direction depend upon the context as above.

In any case, every point $\mathbf{x}$ in the plane has a unique representation

$$\mathbf{x} = u\mathbf{e}_1 + v\mathbf{e}_2 \tag{3.2}$$

for scalars u and v where $v \geq 0$ is the projection onto the eigenmanifold of $\mathbf{e}_2$ along the direction of e_1 and u is the projection onto the eigenmanifold of e_1 along the direction of e_2. We will refer to these (u, v) coordinates as the *natural* coordinates of $\mathbf{x}$ with respect to F.

Now let ℓ_1 and ℓ_2 be the half-lines beginning at $\mathbf{p}$ and running parallel to $\mathbf{e}_1$ and $\mathbf{e}_2$ respectively. We refer to these half-lines as the *eigendirections*. Given a half-line, or *ray*, ℓ, by the notation $\ell \cup -\ell$ we mean the whole line containing ℓ. The *eigenmanifold* of λ_i is the line $\ell_i \cup -\ell_i$, $i = 1, 2$. In terms of the natural coordinates, the plane is divided into four *natural quadrants*, as usual in terms of the signs of u and v.

Let $\mathbf{x} = u_0\mathbf{e}_1 + v_0\mathbf{e}_2$, $v_0 \geq 0$. Then the points $\mathbf{x}_n$ of its orbit under a linear map F corresponding to cases (E_1) or (E_2), are given by

$$\mathbf{x}_n = F^n\mathbf{x} = \lambda_1^n u_0\mathbf{e}_1 + \lambda_2^n v_0\mathbf{e}_2, \qquad n = 0, 1, \ldots,$$

that is, $\mathbf{x}_n$ has the natural coordinates

$$u_n = u_0\lambda_1^n \qquad \text{and} \qquad v_n = v_0\lambda_2^n. \tag{3.3}$$

The analogous equations for a case (E_3) map is derived in §3.6. Note that $u_0 \geq 0$ in cases E_1 and E_2 but it is possible that $u_0 < 0$ in case E_3.

The following is self–evident from equations (3.3).

Proposition 1. *The orbit of a point on an eigenmanifold is contained in the eigenmanifold.*

Proposition 2. *Let the line ℓ contain a flat attractor A, then ℓ is an eigenmanifold for every generating map of A.*

Proof. For contradiction, let F be a locally formative map of A for which ℓ is not an eigenmanifold. Let $\mathbf{p} \in A$ be the fixed point of F and let $\mathbf{x}$ be a point of A distinct from $\mathbf{p}$. Then by assumption, neither natural coordinate of $\mathbf{x}$ is zero, $u_0 \neq 0$ and $v_0 \neq 0$. Since the orbit of $\mathbf{x}$ must also lie on ℓ, the point $\mathbf{x}_1 = h\mathbf{x}$ is a scalar multiple of $\mathbf{x}$, so for some scalar α,

$$\lambda_1 u_0\mathbf{e}_1 + \lambda_2 v_0\mathbf{e}_2 = \alpha(u_0\mathbf{e}_1 + v_0\mathbf{e}_2).$$

Therefore $\lambda_1 = \lambda_2 = \alpha$. But then F is a pure contraction into $\mathbf{p}$ and every line through $\mathbf{p}$ is an eigenmanifold, contradiction. ∎

In the remainder of this section we examine the orbits occurring in spectral cases (E_1)–(E_3).

3.4 *Real Unequal Eigenvalues*

Definition 1. Suppose the eigenvalues to be real and unequal. We distinguish 5 subcases, (a) through (e). First, either $\lambda_2 = -\lambda_1$ or $|\lambda_1| > |\lambda_2|$. We refer to the possibility $\lambda_2 = -\lambda_1$ as subcase (a) the *alternating-similitude* case. The latter possibility, the *differential contractions*, can be further subdivided. Since we have excluded singular maps from consideration, $\lambda_2 \neq 0$, so that in the remaining cases, $|\lambda_1| > |\lambda_2| > 0$. There are 4 possibilities, (b) both eigenvalues are positive, the *exponential* case, (c) the major eigenvalue is positive, the minor negative, the *alternating exponential* case, (d) the major eigenvalue negative, the minor one positive, and (e) both eigenvalues negative.

Proposition 1. *If $|\lambda_1| > |\lambda_2|$ then the orbit for any point $\mathbf{x}$ not on the minor eigenmanifold tends asymptotically to the major eigenmanifold. If in addition $\lambda_1 > 0$ then the orbit lies on one side of the minor eigenmanifold, otherwise it lies on both sides.*

Proof. If $u_0 \neq 0$, then the ratio

$$\frac{v_n}{u_n} = \left(\frac{v_0}{u_0}\right)\left(\frac{\lambda_2}{\lambda_1}\right)^n$$
$$\longrightarrow 0 \qquad \text{as} \qquad n \to \infty$$

It follows that the orbit tends asymptotically to the u axis. By (3.3), if λ_1 is positive, then the sign of u_n remains the same as that of u_0 for all n. Hence, in the natural coordinate system, the orbit remains on the same side of the v-axis as u_0. Otherwise, for $\lambda_1 < 0$, the sign of u_n alternates with each successive n. ∎

Corollary 1. *If $|\lambda_1| > |\lambda_2|$ and $\lambda_1 < 0$, then the orbit can have at most one supporting line at* $\mathbf{p}$.

Since we will only be concerned with those cases for which there is more than one supporting line, this result excludes from consideration subcases (d) and (e).

3.4.1 *Alternating-Similitudes, $\lambda_2 = -\lambda_1$.*

When $\lambda_2 = -\lambda_1$, the even points, $n = 2k$, of an orbit are given by

$$u_{2k} = u_0(\lambda_1^2)^k, \quad \text{and} \quad v_{2k} = v_0(\lambda_1^2)^k, \quad k = 0, 1, \ldots.$$

This is a sequence of points tending to $\mathbf{p}$ along the ray through (u_0, v_0). Similarly the odd points tend to $\mathbf{p}$ along the ray through $(\lambda_1 u_0, -\lambda_1 v_0)$. These rays form a cone at $\mathbf{p}$ and more than one supporting line through $\mathbf{p}$ is possible provided the cone has an acute interior angle over all points $\mathbf{x} = (u_0, v_0) \in A$.

A map with these properties is a true similitude if and only if the eigenmanifolds are orthogonal, otherwise only alternating points behave in true similitude fashion. In the orthogonal case an orbit gives rise to symmetric trajectories about the major eigenmanifold.

Theorem 1. *If $\lambda_2 = -\lambda_1$ then the limbs of the convex hull, c_f and c_b, contain a single orbit.*

Proof. It is easy to see that cones containing orbits nest. ∎

Corollary 2. *In this case the major eigendirection cannot coincide with c_f or c_b.*

Definition 2. Because of the similarity in the treatment of this case and that of the true similitudes, we use the term *extended similitude* to refer to the cases $|\lambda_1| = |\lambda_2|$.

3.4.2 *Exponential Case, $\lambda_1 > \lambda_2 > 0$.*

Definition 3. When the eigenvalues are both positive, then the discrete parametric equations for an orbit (3.3), parameterized for $n = 0, 1, 2, \ldots$ can be extended to the real line, $-\infty < n < \infty$. (For emphasis we may use t in place of n.) The resulting parametric equations for the position vector $\mathbf{x}_t$ give rise to a continuous curve containing the orbit of $\mathbf{x}_0 = (u_0, v_0)$. We call this curve the *trajectory* of (u_0, v_0) under F. When the minor eigenvalue is negative, the trajectory is taken as the curve parameterized by $-\infty < 2n < \infty$.

Now eliminate the parameter n from (3.3),

$$\ln(\frac{u}{u_0}) = n \ln(\lambda_1) \qquad \text{and} \quad \ln(\frac{v}{v_0}) = n \ln(\lambda_2).$$

Hence

$$\frac{\ln(u/u_0)}{\ln(v/v_0)} = \frac{\ln \lambda_1}{\ln \lambda_2} \equiv 1 - \rho. \tag{3.4}$$

So

$$u = u_0 \left(\frac{v}{v_0}\right)^{1-\rho}. \tag{3.5}$$

Proposition 2. *Let the eigenvalues of F satisfy $\lambda_1 > \lambda_2 > 0$. Then the trajectory through any point (u_0, v_0), $u_0 \neq 0$, $v_0 \neq 0$, is an exponential curve with exponent $\ln \lambda_1 / \ln \lambda_2$. If all the points of the attractor lie strictly on one side of the minor eigenmanifold, then the attractor has a cusp at $\mathbf{p}$.*

Proof. The first conclusion follows from (3.5). If all points of the attractor lie strictly on one side of the minor eigenmanifold, then all orbits will be asymptotic to one ray of the major eigenmanifold. ∎

Remark. Since (3.5) is single valued, trajectories are either disjoint or identical with the common limit point $\mathbf{p}$.

3.4.3 *Alternating Exponential Case.*

In case $\lambda_1 > 0$ and $\lambda_2 < 0$, the even orbit points $\mathbf{x}, F^2\mathbf{x}, \ldots$ work just as above except with effective eigenvalues of λ_1^2 and λ_2^2. The odd orbit points also behave as above but occur on the opposite side of the v axis with squared eigenvalues. Hence in this case there is a cusp at the fixed-point along the positive u axis and consequently multiple supporting lines can exist.

3.5 *Equal eigenvalues, linearly independent eigenvectors – Non-Rotational Similitude.*

Let $\mathbf{e}_1$ and $\mathbf{e}_2$ be two linearly independent eigenvectors and let λ be their common eigenvalue. Let $\mathbf{x} = u_0\mathbf{e}_1 + v_0\mathbf{e}_2$ be any point. Then $F\mathbf{x} = u_0\lambda e_1 + v_0\lambda e_2 = \lambda\mathbf{x}$. Hence F is a contraction by λ in each direction in this case, i.e. a non-rotational similitude. The orbits

will lie on straight lines through the fixed-point. There are two subcases, $\lambda > 0$ and $\lambda < 0$. In the latter, the orbit lies on both sides of the fixed point and hence there can be at most one supporting line, thus we may eliminate the subcase $\lambda < 0$ from consideration.

3.6 *Geometrical Multiplicity One (GM-1) Case, $\lambda_2 = \lambda_1$.*

By Jordan Canonical Form, F can be written as

$$\begin{pmatrix} \lambda & \gamma \\ 0 & \lambda \end{pmatrix}. \tag{3.6}$$

for a basis $\mathbf{e}_1$, $\mathbf{e}_2$ where the former is an eigenvector for the eigenvalue λ and the latter is orthogonal to the first. We may choose $\mathbf{e}_2$ so that γ is positive, but since $\mathbf{e}_2$ is normalized, γ is not necessarily 1. Now let $\mathbf{x}$ be a given vector. If $\mathbf{x} = u_0\mathbf{e}_1$, then the orbit $\{F^n\mathbf{x} = u_0\lambda^n\mathbf{e}_1 \ : \ n = 0, 1, \ldots\}$ is a geometric sequence along the line through $\mathbf{e}_1$. The sequence confines itself to the positive (or negative) side of the u-axis if and only if $\lambda > 0$. Otherwise suppose $\mathbf{x} = u_0\mathbf{e}_1 + v_0\mathbf{e}_2$, $v_0 \neq 0$. Then by trivial induction,

$$F^n\mathbf{x} = \lambda^n v_0\mathbf{e}_2 + (n\lambda^{n-1}v_0\gamma + \lambda^n u_0)\mathbf{e}_1, \quad n = 0, 1, \ldots.$$

In parametric equations

$$\begin{aligned} u_n &= n\lambda^{n-1}v_0\gamma + \lambda^n u_0, \qquad n = 0, 1, \ldots \\ v_n &= \lambda^n v_0 \end{aligned} \tag{3.7}$$

Proposition 1. *Orbits of an affine map with equal eigenvalues and only one linearly independent eigenvector tend asymptotically to the major eigenmanifold (the u-axis).*

Proof. Clearly u_n and v_n tend to 0 as $n \to \infty$. Moreover the ratio $|v_n/u_n|$ is given by

$$\left|\frac{v_n}{u_n}\right| = \frac{|v_0|}{|n\gamma(v_0/\lambda) + u_0|}$$

and is $O(1/n)$ (harmonic) for $n \to \infty$. ∎

Geometrical Multiplicity One (GM-1) Trajectory

If $\lambda < 0$, then unless $v_0 = 0$ (that is the attractor is flat), $n\lambda^{n-1}v_0$ dominates $\lambda^n u_0$ in (3.7) and this term changes in sign with n. Hence so does u_n. Similarly $v_n = v_0\lambda^n$ changes in sign with n and so for large n, u_n and v_n are opposite signed and alternate in sign. Since the orbit is at the same time asymptotic to the u-axis, it follows that there can be no supporting line at the fixed point and so this possibility is excluded from consideration.

Now suppose $\lambda > 0$ and consider the sign of v_0. If $v_0 > 0$ then from (3.7) both v_n and (for large n) u_n are positive and so the orbit approaches the u-axis from the first quadrant. But if $v_0 < 0$, then both v_n and (eventually) u_n will be negative and now the orbit tends to the u-axis from the third quadrant. It follows that in this case, points of the attractor cannot lie on both sides of the u-axis, and proves the following.

Proposition 2. *The major eigenmanifold must be a supporting line of the attractor in this case.*

For $\lambda > 0$, we may consider n to be a continuous variable, $-\infty < n < \infty$, and equations (3.7) as the parametric equations of a curve. From the second equation in (3.7), $n = (\ln v - \ln v_0)/\ln\lambda$. From the first equation,

$$\begin{aligned} u &= \frac{n\lambda^n v_0\gamma}{\lambda} + \lambda^n v_0 \frac{u_0}{v_0} = \frac{nv\gamma}{\lambda} + \frac{u_0}{v_0} v \\ &= \left(\frac{\gamma}{\lambda\ln\lambda}(\ln v - \ln v_0) + \frac{u_0}{v_0}\right) v \\ &= \left[\left(\frac{u_0}{v_0} - \frac{\gamma\ln v_0}{\lambda\ln\lambda}\right) + \frac{\gamma}{\lambda\ln\lambda}\ln v\right] v \\ &= (a + b\ln v)v, \end{aligned} \tag{3.8}$$

where the constants a and b are given by

$$a = \frac{u_0}{v_0} - \frac{\gamma\ln v_0}{\lambda\ln\lambda} \qquad \text{and} \qquad b = \frac{\gamma}{\lambda\ln\lambda}. \tag{3.9}$$

From (3.7) the slope of the secant line segment joining the origin $(0,0)$ to the point (u,v) is given by

$$\frac{u}{v} = a + b\ln v.$$

Since $b \neq 0$, this slope tends monotonically to $\pm\infty$ as v tends to 0 (for sufficiently small v). Hence, once again, the attractor will have a cusp at $\mathbf{p}$ along the major eigenmanifold if all points of the attractor lie strictly above the minor eigenmanifold. Consequently multiple supporting lines are possible in this case.

3.7 *Summary*

We collect here some observations of the previous subsections. Coordinates refer to fig. 2.

Theorem 1. *Let F be locally formative for the 2-dimensional attractor A and have fixed point $\mathbf{p}$. Assume the eigenvalues of F are distinct.*
(a) If A is flat, then it is parallel to an eigenmanifold of F.
(b) If A is not flat, then the major eigenvalue of F is positive, $\lambda_1 > 0$, the major eigenmanifold, ℓ_1, of F meets the deleted convex hull $C_A - \{\mathbf{p}\}$ of A, $arg(\ell_1) \leq \arg(c_b)$, and the minor eigenmanifold, ℓ_2 meets at most the boundary ∂C_A of C_A, that is $\arg(\ell_2) = 0$ or $\arg(\ell_2) \geq \arg(c_b)$.

Proof. The only undemonstrated assertions are those about the major and minor eigenmanifolds of F. For the major eigenmanifold, suppose the assertion is false. Since the

orbit for any $\mathbf{x}$ not lying on ℓ_2 tends asymptotically to ℓ_1, points of the orbit of such an $\mathbf{x}$ must lie in every positive cone centered at ℓ_1, in particular the cone of half-angle $\frac{1}{2}(\arg(\ell_1) - \arg(c_b))$. This contradicts that c_b supports A.

For the minor eigenmanifold, suppose not. Then there are points of the attractor $\mathbf{x}$ and $\mathbf{y}$ lying on both sides of $\ell_2 \cup -\ell_2$. By the analysis of this section, one will tend to ℓ_1 and the other to the opposite side, $-\ell_1$. Hence the line $\ell_1 \cup -\ell_1$ can be the only supporting line through $\mathbf{p}$. This contradicts that $\mathbf{p}$ is an extreme point. ∎

Corollary 1. *Relative to the natural coordinate system at* $\mathbf{p}$*, all points of the attractor have non-negative u coordinate, that is the entire attractor lies on one side of the minor eigenmanifold, the first or fourth quadrants or both.*

Proof. The minor eigenmanifold is a supporting line for the attractor at $\mathbf{p}$ and therefore all points of the attractor have either non-negative or non-positive coordinates. Since the positive u axis is inside or on the hull of A, the coordinates are non-negative. ∎

Corollary 2. *With hypothesis as above, unless* ℓ_2 *coincides with one of* c_f *or* c_b*, A has a cusp at* $\mathbf{p}$*.*

Proof. All points of the attractor have positive u coordinate, and therefore tend asymptotically to ℓ_1. ∎

Theorem 2. *In every case trajectories are single valued as parameterized by the minor natural coordinate* v*. Hence the natural coordinate* v *may be taken as the trajectory parameter,* $u = \mathbf{t}(v)$*.*

The results of this section may be summarized in the following table which correlates the spectral nature of a map with the geometrical properties of its orbits near its fixed point. Note that only in the cases: alternating-similitude, rank one, exponential, alternating exponential, and non-rotational similitude can the fixed point also be an extreme point of the attractor.

eigenvalues	designation	orbital geometry	springbar type
non-primary			
complex	no primary points	spirals	–
$\lambda_1 < 0$, $\lambda_2 < 0$	no primary points	locally sigmoid	–
$\lambda_1 < 0$, $\lambda_2 > 0$	no primary points	locally convex	–
extended similitudes			
$\lambda_2 = -\lambda_1$	alternating-similitude	wedge, no cusp	asy. const.
$\lambda_2 = \lambda_1$, 2 e-vect.	non-rot. similitude	wedge, no cusp.	asy. const.
differential contractions			
$\lambda_1 > 0$, $\lambda_2 > 0$	exponential	cusp/wedge	mono./const.
$\lambda_1 > 0$, $\lambda_2 < 0$	alt. exponential	cusp, no wedge	strictly mono.
geometrical multiplicity one (GM-1)			
$\lambda_2 = \lambda_1$, 1 e-vect.	harmonic	cusp, no wedge	strictly mono.

Table 1

4 Polar Coordinate Representations

The most readily accessible trajectory is the one which constitutes the edge or margin of an attractor. In the next section we introduce a tool, the *springbar function*, for finding it. We show that from the resulting polar coordinate plot, enough can be learned to enable the construction of arbitrary trajectories. In this section we lay the groundwork for these plots by calculating the polar coordinate plots for the several spectral cases

In this section we assume that $\mathbf{p}$ is the extreme fixed point of the formative or locally formative map F.

4.1 *Polar Representation of Trajectories by Case*

Initially the eigendirections are unknown, hence it is preferable to recast the trajectories of §3 in terms of a local polar coordinate system. Distance r is measured from $\mathbf{p}$ and angles θ are measured from the forward limb of the convex hull, see fig. 2 §3.2. In this section we obtain the polar form of the trajectory curves for each spectral case. Note that the alternating cases follow their non-alternating counterparts but with the square of their eigenvalues.

4.1.1 *Positive Refinement for Alternating Cases*

Let $\mathcal{W} = \{w_1, w_2, \ldots, w_N\}$ be an *IFS* for A with a (globally) formative map w_1 whose minor eigenvalue is negative. The partial refinement

$$\mathcal{W}' = \{w_1 w_1, w_1 w_2, \ldots, w_1 w_N, w_2, \ldots, w_N\}$$

is an equivalent *IFS* for A since $w_1(A) = \cup_1^N w_1 w_i(A)$. But now the eigenvalues of w_1^2 are both positive. The additional maps, $w_1 w_i$, $i \neq 1$, are decorative. In this way we replace all formative maps in $\mathcal{W}$ having negative minor eigenvalue, by its subtile partial refinement one by one and thereby arrive at an equivalent *IFS* for the attractor for which the alternating cases do not occur for the formative maps. Thus $\mathcal{W}'$ is the *positive refinement* of $\mathcal{W}$.

Likewise, by ignoring the alternating cases for locally formative maps, the spectral types of their squares will match the appropriate formative generating map in the positive refinement $\mathcal{W}'$. Hence we no longer have to treat the alternating cases nor extended similitudes.

In order to obtain a minimal *IFS* solution, one should discriminate for negative minor eigenvalues. However from the foregoing it is not necessary to do so. Nevertheless it is possible to test for the alternating case. We leave it to the reader to develop these tests.

In the sequel we will assume this positive refinement has been done and that all eigenvalues are non-negative.

4.1.2 *Extended Similitudes,* $\lambda_2 = \lambda_1$.

In this case F is exactly λI with only one unknown parameter, λ. Trajectories of F are rays emanating from the fixed–point $\mathbf{p}$ and have the polar form

$$\theta = \text{constant}.$$

4.1.3 *Differential Contractions,* $\lambda_1 > \lambda_2 > 0$.

In natural coordinates an exponential trajectory is given from eq.(3.5) by

$$u = u_0 \left(\frac{v}{v_0} \right)^{1-\rho}. \tag{4.1}$$

To convert this to polar coordinates, let r be as above and let ϕ measure the angle from ℓ_1, the u axis, $\phi = |\theta - \arg(\ell_1)|$. Recall from §3.4 that ℓ_1 is the trajectory asymptote and therefore is known, see fig. 3. Let ω be the angle between the eigenvectors $\mathbf{e}_1$ and $\mathbf{e}_2$ and let $\omega' = \pi - \omega$, see fig. 3.

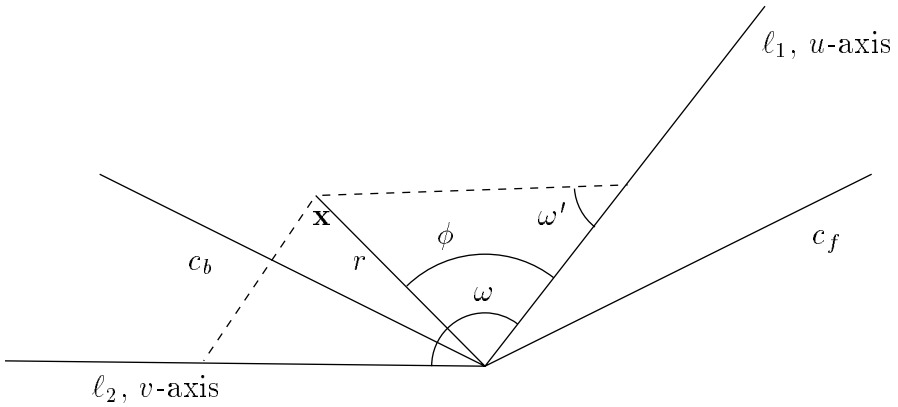

fig. 3

By the Law of Sines

$$\frac{v}{\sin\phi} = \frac{r}{\sin\omega'} \tag{4.2}$$

and by the Law of Cosines

$$r^2 = u^2 + v^2 - 2uv\cos\omega'. \tag{4.3}$$

Therefore substituting (4.2) into (4.1) gives u in polar coordinates

$$u = \frac{u_0}{v_0^{1-\rho}}\left(\frac{r\sin\phi}{\sin\omega'}\right)^{1-\rho}.$$

Hence equation (4.2) for r becomes

$$r^2 = u_0^2\left(\frac{\sin^2\phi}{v_0^2\sin^2\omega'}\right)^{1-\rho}(r^2)^{1-\rho} + \frac{r^2\sin^2\phi}{\sin^2\omega'} - 2u_0\left(\frac{\sin\phi}{v_0\sin\omega'}\right)^{1-\rho} r^{1-\rho} r\frac{\sin\phi}{\sin\omega'}\cos\omega'.$$

Divide by r^2 $(r \neq 0)$

$$1 = u_0^2\left(\frac{\sin^2\phi}{v_0^2\sin^2\omega'}\right)^{1-\rho} r^{-2\rho} + \frac{\sin^2\phi}{\sin^2\omega'} - \frac{2u_0}{v_0^{1-\rho}}\left(\frac{\sin\phi}{\sin\omega'}\right)^{2-\rho}(\cos\omega')r^{-\rho}.$$

This is quadratic in $r^{-\rho}$

$$u_0^2\left(\frac{\sin^2\phi}{v_0^2\sin^2\omega'}\right)^{1-\rho}(r^{-\rho})^2 - \frac{2u_0\cos\omega'}{v_0^{1-\rho}}\left(\frac{\sin\phi}{\sin\omega'}\right)^{2-\rho}(r^{-\rho}) + \left(\frac{\sin^2\phi}{\sin^2\omega'} - 1\right) = 0.$$

Solve for $r^{-\rho}$ by the quadratic formula. It may be verified that the solutions are

$$r^{-\rho} = \frac{v_0^{1-\rho} \sin^{-\rho} \omega'}{u_0 \sin^{1-\rho} \phi} \sin(\phi \pm \omega').$$

Since r is always positive, (assume ϕ is positive, choose the v axis always on the side of the trajectory) then we must choose the + sign because ϕ can tend to 0. The solution for r is

$$r = \left(\frac{u_0}{v_0^{1-\rho}}\right)^{1/\rho} \sin\omega' \left(\frac{\sin^{1-\rho}\phi}{\sin(\phi+\omega')}\right)^{1/\rho}. \tag{4.4}$$

As ϕ tends to 0 (at the asymptote)

$$\frac{\sin^{1-\rho}\phi}{\sin(\phi+\omega')} \longrightarrow \frac{\phi^{1-\rho}}{\sin\omega'}$$

and therefore r tends to

$$r = \frac{\sin\omega'}{\sin^{1/\rho}\omega'} \left(\frac{u_0}{v_0^{1-\rho}}\right)^{1/\rho} \phi^{\frac{1-\rho}{\rho}} = \frac{(u_0/v_0^{1-\rho})^{1/\rho}}{(\sin\omega')^{\frac{1}{\rho}-1}} \phi^{\frac{1}{\rho}-1}.$$

Taking logarithms

$$\ln r = \ln\left(\frac{(u_0/v_0^{1-\rho})^{1/\rho}}{(\sin\omega')^{\frac{1}{\rho}-1}}\right) + \left(\frac{1}{\rho}-1\right)\ln\phi \tag{4.5}$$

asymptotically as $\phi \to 0$.

Theorem 1. *Let F be locally formative for A at $\mathbf{p}$ with distinct eigenvalues, $\lambda_1 > \lambda_2 > 0$. Let ω be the angle between their eigenvectors and let $\rho = \frac{\ln\lambda_1}{\ln\lambda_2}$. For any point $\mathbf{x}$ of A not lying on an eigenmanifold of F, the graph of $\eta = \ln r$ versus $\xi = \ln\phi$ for the trajectory through $\mathbf{x}$ tends asymptotically to a straight line as $\xi \to -\infty$. If m and b are the slope and intercept respectively of this line, then*

$$m = \frac{1}{\rho} - 1 \tag{4.6}$$

and

$$e^b = \frac{(u_0/v_0^{1-\rho})^{1/\rho}}{(\sin\omega)^{\frac{1}{\rho}-1}} \tag{4.7}$$

from which ρ and ω can be determined.

Proof. This is a summary of above.

4.1.4 *Geometrical Multiplicity One (GM-1),* $\lambda_2 = \lambda_1$.

In this case the natural coordinates (u, v) measure distances along, respectively, the asymptote and an axis orthogonal to it. Further the trajectory is given by (3.8)

$$u = (a + b \ln v)v \tag{4.8}$$

where

$$b = \frac{\gamma}{\lambda \ln \lambda}, \quad \text{and} \quad a = \left(\frac{u_0}{v_0} - \frac{\gamma \ln v_0}{\lambda \ln \lambda} \right). \tag{4.9}$$

Since the asymptote lies along the boundary of the convex hull in this case, ϕ and θ are the same (at least if the asymptote lies along the forward limb).

Change to polar coordinates, as above $\phi = |\theta - \arg(\ell_1)|$,

$$v = r \sin \phi$$

and

$$\begin{aligned} r^2 &= v^2 + u^2 \\ &= r^2 \sin^2 \phi (1 + (a + b \ln(r \sin \phi))^2). \end{aligned}$$

Solve for $\ln r$,

$$\frac{\sqrt{(\frac{1}{\sin^2 \phi} - 1)} - a}{b} = \ln r + \ln(\sin \phi).$$

For ϕ near 0 the left hand side tends to

$$\frac{1}{b\phi},$$

and the right to $\ln r + \ln \phi$. Hence, asymptotically,

$$\begin{aligned} \ln r &= \frac{1}{b\phi} - \ln \phi \\ &= \left(\frac{\frac{1}{b}}{\phi \ln \phi} - 1 \right) \ln \phi. \end{aligned}$$

As $\phi \to 0$, $\frac{1}{\phi \ln \phi} \to \infty$. Therefore the graph of $\ln r$ vs $\ln \phi$ does not tend to a straight line; rather its slope tends to $+\infty$.

Theorem 2. *In log polar coordinates, the slope of a GM-1 trajectory tends to* $+\infty$ *as* r *(and* ϕ*) tend to 0. Hence this case is distinguished from the exponential case by their respective* $\ln r$ *vs* $\ln \phi$ *graphs.*

5 Springbar Function

From the previous two sections we know the character of trajectories for a given type of map. Conversely, from the character of the attractor at an extreme point $\mathbf{p}$ we can calculate the locally formative map. In this section we show how to do this up to a single scalar parameter. This is sufficient for calculating a trajectory through a given point.

5.1 *Supporting Trajectories*

Definition 1. By a *trajectory family* at an extreme point $\mathbf{p}$ we mean the collection of trajectories $\mathbf{t}_{\mathbf{x}_0}(\cdot)$, one for each initial point $\mathbf{x}_0 \in A$, corresponding to some locally formative map F at $\mathbf{p}$. Thus a trajectory family is given in natural coordinates by

$$u = \mathbf{t}_{\mathbf{x}_0}(v) = u_0 \left(\frac{v}{v_0}\right)^{1-\rho}, \quad v \geq 0 \tag{5.1a}$$

if F is a differential contraction or by

$$u = \mathbf{t}_{\mathbf{x}_0}(v) = \frac{u_0}{v_0} v, \qquad v \geq 0 \tag{5.1b}$$

if F is an extended similitude or by

$$u = \mathbf{t}_{\mathbf{x}_0}(v) = (a + b \ln v)v, \qquad v \geq 0 \tag{5.1c}$$

with constants a and b as in §3.6 if F is of geometrical multiplicity one.

Definition 2. By the *trace* of a trajectory we mean its intersection with the attractor. A trace is *complete* if it has the extreme point $\mathbf{p}$ as a limit point, otherwise it is *void*.

Definition 3. The *domain of invariance* of a trajectory family is the set of points $\mathbf{x}_0 \in A$ whose trajectories have a complete trace.

Definition 4. Let $\mathbf{t}_1$ and $\mathbf{t}_2$ be two trajectories of some trajectory family at $\mathbf{p}$ for $\mathbf{x}_1$ and $\mathbf{x}_2$ respectively having complete traces. If they lie in the same (natural) quadrant, we say $\mathbf{t}_1$ is *below* $\mathbf{t}_2$, $\mathbf{t}_1 \prec \mathbf{t}_2$, if $\mathbf{t}_1(v) \leq \mathbf{t}_2(v)$, $0 < v < \infty$. Two trajectories lying in different quadrants are not comparable.

Definition 5. If points of the attractor occupy two natural quadrants, then the *supporting trajectory* in each is the minimal trajectory with respect to this partial order, see fig 4. If the attractor lies in only one natural quadrant at $\mathbf{p}$ with respect to a locally formative map, then the two supporting trajectories are the minimum and the maximum trajectories with respect to this partial order. Treat trajectories lying along the u-axis as the limiting case of trajectories from within the quadrant.

Remark. *The supporting trajectory for the frond of the fern, fig. 11, runs along the frond itself and not along the convex hull since the latter is not a trajectory from the domain of invariance of the trajectory family.*

Theorem 1. *If the attractor A contains a point lying strictly on one side of the major eigendirection, ℓ_1, of F, then A has a supporting trajectory on that side.*

Proof. Let $\mathbf{x}$ be a point of the attractor not lying on ℓ_1, say the v coordinate of $\mathbf{x}$ is positive the other case being similar. Let m be a line through $\mathbf{x}$ parallel to ℓ_1. For every point $\mathbf{a} \in A$ in the first quadrant, let u_a be the point on m where the trajectory through $\mathbf{a}$ intersects m. The set of all such u_a is bounded below and so has an infimum, u^*. Then e^*, the trajectory of F through u^*, evidently supports A. It remains to show that e^* is the trajectory of some point of A.

For $\delta = 2^{-n}$ let e_n be a trajectory of A whose intersection u_n with m is within δ of u^*. The mapping which sends $u_n \mapsto e_n$ to its trajectory is a homeomorphism.

Let $\mathbf{a}_n$ be the point of A on e_n most distant from the fixed point $\mathbf{p}$. The set $\{\mathbf{a}_n : n = 1, 2, \dots\}$, as an infinite subset of the compact set A, must have a limit point in A, say $\mathbf{a}^*$. Observe that the points $\mathbf{a}_n$ are bounded away from $\mathbf{p}$. This is because $\mathbf{p}$ lies in the secondary tile $F^2(A)$ and since $\mathbf{a}_n$ is the most distance attractor point on an orbit, it can't be in $F^2(A)$ as all these points are images under F of some more distant point of A.

Since the points $\mathbf{a}_n$ are bounded away from $\mathbf{p}$, the limit point $\mathbf{a}^*$ is not $\mathbf{p}$ and therefore generates an orbit. By the homeomorphism, its trajectory likewise has a limit point on m. But the only one is u^*. Hence the trajectory is exactly e^*. ∎

Definition 6. Let $\mathbf{t}^*$ be a supporting trajectory of A at $\mathbf{p}$. Its trace will be referred to as a *margin* of A at $\mathbf{p}$.

5.2 *Springbar Functions*

The most readily accessible trajectory is the one which constitutes the edge of an attractor. In this section we introduce a tool, the *springbar function*, for finding it. We show that from the resulting polar coordinate plot, enough can be learned to enable the construction of trajectory families.

Definition 1. Let $\mathbf{p}$ be an extreme point of the attractor A and let $\mathbf{p}'$ be the adjacent extreme point on the convex hull C_A counterclockwise from $\mathbf{p}$. Let r measure Euclidean distance from $\mathbf{p}$ and for each $r > 0$ let $\alpha = \alpha(r)$ be defined by

$$\alpha = \inf\{\arg(\mathbf{x}) \,:\, \mathbf{x} \in A \cap \overline{B}_{\mathbf{p}}(r)\}$$

where $\arg(\mathbf{x})$ is measured from the line through $\mathbf{pp}'$ to the line $\mathbf{px}$ and $B_{\mathbf{p}}(r)$ is the ball of radius r around $\mathbf{p}$. We refer to the function α so defined as the *forward springbar*

fig. 4, Supporting Trajectories

function. It has the following properties: (1) the infimum is attained, (2) α is monotone non-increasing with values from 0 to π, and, due to the use of the closed ball, (3) α is right continuous.

Analogously we define the *backward springbar function* $\beta = \beta(r)$ by

$$\beta = \sup\{\arg(\mathbf{x}) \,:\, \mathbf{x} \in A \cap \overline{B}_{\mathbf{p}}(r)\}$$

where $\arg(\mathbf{x})$ is measured as above. The properties of β are the same as above except that β is monotone non-decreasing and need not attain the value 0.

The small crosses in fig. 4 are points of the attractor upon which the springbar has come to rest.

Put the two together in one plot with α to the right along the positive abscissa and β to the left along the negative abscissa. Either way, r increases away from the origin. We call this the *springbar plot* at $\mathbf{p}$.

There is a close connection between the supporting trajectories at $\mathbf{p}$ and the forward and backward springbar functions.

Proposition 1. *Infinitely many points of the margin on the forward supporting trajectory lie in the graph of the forward springbar function. Between any two such points, the forward springbar function lies above or on the polar coordinate representation of the forward supporting trajectory. Similar statements hold for the backward springbar function and the backward supporting trajectory.*

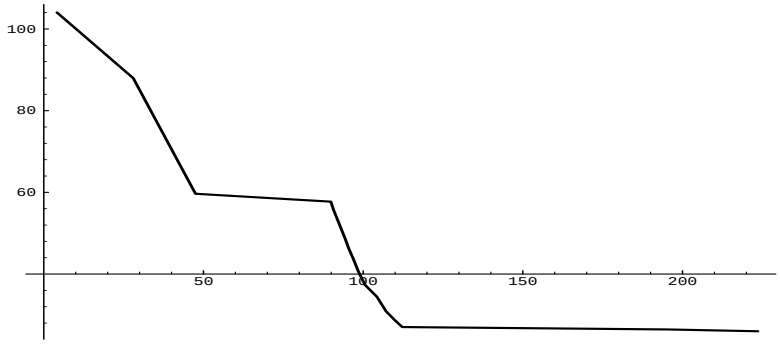

fig. 5, Forward Springbar Function for fig. 4

Proof. Since the supporting trajectory is a trajectory from the domain of invariance, there are attractor points on it inside every deleted ball. By the disjointness of tiles, there is a ball of some positive radius, $r_0 > 0$, such that the only points of the attractor inside this ball also belong to the tile containing $\mathbf{p}$. Hence for $r \leq r_0$, the springbar will either come to rest on a point of the margin or on a point in the domain of invariance whose trajectory is interior to the supporting trajectory. This proves that the springbar function for $r \leq r_0$ lies above or on the polar coordinate plot of the supporting trajectory. On the other hand, since all three types of supporting trajectories are convex, every point of the margin with radius r_0 must also lie on the springbar plot. ∎

5.3 *Trajectory Family Determination*

In this subsection we determine, for the most part uniquely, the trajectory family at an extreme point $\mathbf{p}$ by relating the geometry at $\mathbf{p}$ to the three spectral cases and the additional subcases resulting from the interplay between the eigenmanifolds and the convex hull. The purpose is to justify the orbital geometry and springbar types columns of Table 1 of §3.6.

5.3.1 *Non-rotational Similitude, $\lambda_2 = \lambda_1$.*

Since the trajectories are rays, in a small enough neighborhood of $\mathbf{p}$ the attractor will be wedge–shaped, cf. the fronds of the fractal fern fig 11. Hence the springbar plot will be two–sided constant if F is globally formative, or two–sided asymptotically constant if F is only locally formative. There will be a jump discontinuity at the origin equal to the interior angle between supporting trajectories at $\mathbf{p}$, the wedge angle. The trajectory family in this case is (5.1b).

Every direction in this case is an eigendirection, and therefore there are no subcases to deal with here arising from an interplay between the convex hull and the eigenmanifolds.

Note that while the contraction factor of a non-rotational similitude is evident in its orbits, that information is lost in its trajectories, hence the springbar plot cannot determine the contraction factor.

5.3.2 *Exponential,* $\lambda_1 > \lambda_2 > 0$.

There are four subcases here depending on the relationship between the eigenmanifolds and the limbs of the convex hull at $\mathbf{p}$: (a) neither coincides with the boundary, (b) ℓ_1 lies on ∂C_A but ℓ_2 does not, (c) ℓ_2 lies on ∂C_A but ℓ_1 does not, or (d) both coincide with the boundary (False Similitude case).

If neither eigendirection lies on ∂C_A, the supporting trajectory on each side of ℓ_1 will be an exponential curve (see §3.4); hence there is a two-sided cusp in this case, as in fig. 4. The forward springbar function is monotonically decreasing and reaches 0 when r equals the distance to the next extreme point $\mathbf{p}'$. As $r \to 0$, $\alpha(r) \to \arg(\ell_1)$, see fig. 5. The backward springbar function is monotonically increasing and tends to the interior angle of the convex hull at $\mathbf{p}$. Hence the plot is continuous at the origin.

If the major eigendirection lies on ∂C_A but the minor does not, then that boundary of the hull itself will be a straight line supporting trajectory while on the other side it will be an exponential curve. Hence there will be a cusp at $\mathbf{p}$, and consequently the springbar function is constant on one side and monotonic on the other. Again the springbar plot is continuous at the origin in this case. We summarize these facts in the following Proposition.

Proposition 1. *In subcases (a) and (b) there is a cusp at* $\mathbf{p}$ *and the springbar plot is continuous at the origin,*

$$\lim_{r \to 0} (\alpha(r) - \beta(r)) = 0.$$

If the minor eigendirection lies on ∂C_A but the major one does not, then again the boundary of the convex hull itself will be a straight line supporting trajectory while the other side will be an exponential curve asymptotically tangent to the major eigendirection. However this time there will be an asymptotic wedge at $\mathbf{p}$, instead of a cusp, equal to the angle ω between the major and minor eigendirections. The springbar plot will have a jump discontinuity at the origin equal to this angle.

Proposition 2. *In subcase (c) there is an exponential wedge at* $\mathbf{p}$,

$$\lim_{r \to 0} (\alpha(r) - \beta(r)) = \omega > 0$$

where the wedge angle ω *is the angle between the eigenmanifolds at* $\mathbf{p}$.

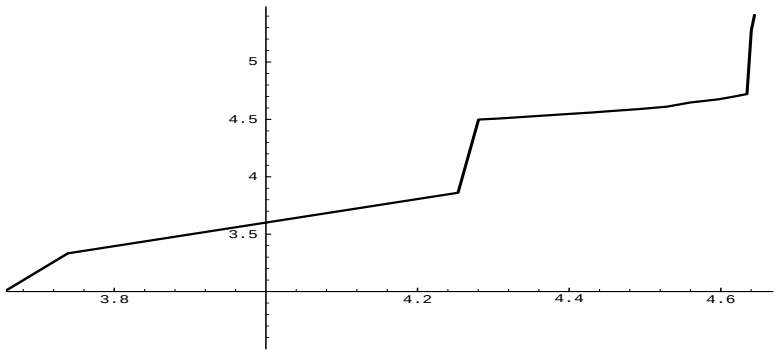

fig. 6, Log-log plot of the Springbar Function of fig. 5

If both eigenmanifolds lie on ∂C_A, then both supporting trajectories will be the straight lines of the boundary of the convex hull and the springbar functions will be constant with a jump discontinuity at the origin. Unfortunately this is also the signature of an extended similitude case as we have seen above. Therefore we will have to discriminate the two cases in some other fashion than by their springbar plot (see §5.3). We refer to this as the *False Similitude* case.

Calculating the Trajectory Family for an Exponential Extreme Point

We have seen in this case that the springbar curve lies above the polar form of the supporting exponential trajectory except where the two have a common value, that is touch. Moreover they touch infinitely often corresponding to a geometric sequence in their minor natural coordinate since every point $\mathbf{x}$ lying on such a trajectory, generates an entire orbit contained in that trajectory.

The same will be true of their respective log-log plots. More precisely, since the cusp angle $\arg(\ell_1)$ can be observed in this case, we may form the plot of $\eta = \ln(\arg(\ell_1) - \alpha)$ versus $\xi = \ln r$ for a forward springbar plot (or a plot of $\ln(\beta - \arg(\ell_1))$ versus $\ln r$ for a backward springbar plot) and compare with their supporting trajectory counterpart. From the observations of §4.1, the log-log trajectory plot tends asymptotically to a straight line with slope $M = 1/m$ and intercept $B = -b/m$ to use the notation of equations (4.6) and (4.7), see fig. 6. Moreover the log-log springbar plot lies above the trajectory plot but touches it almost periodically. These considerations yield the following theorem and procedure for calculating the slope M and intercept B.

Theorem 1. *For $x < 0$ and $y < \eta(x)$ let $\ell(x, y, M)$ denote the ray on $-\infty < \xi \leq x$ through (x, y) and having slope $M > 0$. Let*

$$M(x, y) = \inf\{M \ : \ \ell(x, y, M) \text{ lies below } \eta(\xi), \xi \leq x\},$$

and let

$$M(x) = \lim_{y \to -\infty} M(x, y).$$

$M(x)$ is constant for all x, say equal to M^*. Let

$$y(x) = \sup\{y \,:\, \ell(x, y, M^*) \text{ lies below } \eta(\xi),\ \xi \le x\}.$$

Finally let $B(x)$ denote the intercept of the extension of $\ell(x, y(x), M^*)$, then

$$B = \lim_{x \to -\infty} B(x).$$

Proof. By previous results the springbar curve lies above the polar plot and the latter tends to a line. That both limits above exist follows from the observation that the function $M(x, y)$ is monotone in y and the function $B(x)$ is monotone in x. ∎

Corollary 1. *The parameters m and b of (4.6) and (4.7) are given by*

$$m = \frac{1}{M} \qquad \text{and} \qquad b = -mB.$$

In turn, the parameters ρ of (5.1a) and the angle ω between the major and minor eigendirections are given by

$$\rho = \frac{1}{m+1} \qquad \text{and} \qquad \sin\omega = \frac{(u_0\, e^{-b\rho})^{1/(1-\rho)}}{v_0}.$$

Hence in this case both eigendirections can be calculated.

Proof. These statements follow from the cited equations. ∎

5.3.3 *Geometrical Multiplicity One, GM-1, $\lambda_2 = \lambda_1$.*

In this case the single eigendirection lies on ∂C_A, Proposition 3.6.2, and so the limb of the convex hull on that side will be a straight line supporting trajectory. On the other side there will be a harmonic supporting trajectory. Hence the attractor will have a cusp at **p**.

Having distinguished this case from that of a differential contraction by the unbounded slope in this case of the $\log r$ versus $\log\phi$ springbar plot, Theorem 4.1.2, it remains to solve for the matrix parameters γ and λ, (3.6).

As in the differential contraction case, the springbar plot will lie above the polar coordinate graph of the harmonic supporting trajectory and touch it infinitely often as $r \to 0$. It follows likewise that the natural coordinate (u, v) plot of the springbar function also lies above that of the supporting trajectory. Hence for a given value of v, the springbar value of u exceeds or equals that of the harmonic supporting trajectory (when u exists)

and so the springbar plot of $\eta = \frac{u}{v}$ versus $\xi = \ln v$ lies above the corresponding graph of the harmonic supporting trajectory and the two touch infinitely often as $\xi \to -\infty$.

Now the η versus ξ trajectory graph is a straight line with slope $b = \gamma/(\lambda \ln \lambda) < 0$ and intercept $a = \frac{u_0}{v_0} - b \ln v_0$, (3.9). Therefore by fitting a line from below to this η versus ξ springbar plot the parameters a and b can be calculated. We summarize all this in the following theorem.

Theorem 2. *In the GM-1 case the unknown parameters a and b may be calculated by fitting a straight line from below to the springbar plot of $\eta = u/v$ versus $\xi = \ln v$.*

It follows that here as in the other cases, enough information is available from the springbar plot to enable the calculation of arbitrary trajectories parameterized by the minor natural coordinate v. In the next section we show how to calculate λ from the pattern of points lying on such a trajectory. Then γ is found from

$$\gamma = b\lambda \ln \lambda. \tag{5.2}$$

5.4 *Summary*

Theorem 1. *With the exception of the False Similitude case, trajectories are uniquely determined by the local geometry. That is, the locally formative map is determined to within a scalar parameter such that given an initial point $\mathbf{x}_0$, the trajectory through $\mathbf{x}_0$ can be calculated.*

Proof. The existence of a cusp at $\mathbf{p}$ implies the locally formative map be either a differential contraction or of GM-1. The shape of the cusp uniquely determines which and moreover uniquely determines the trajectory parameters. Except for the False Similitude possibility, the absence of a cusp implies a similitude case. ∎

Remark. *See fig 16 for an example in the False Similitude case where the locally formative map can be either a differential contraction or a similitude.*

6 Gap Analysis

The techniques of the last section enable one to calculate trajectory mapping functions for the locally formative map at each extreme point of the convex hull. However trajectories are not orbits. One scalar parameter separates the two, for instance, knowledge of the minor eigenvalue, which, when combined with the trajectory information, completely determines the locally formative map.

Therefore we have reduced the problem to one dimension, and in fact, for one dimensional attractors, all of which may be interpreted as non-rotational similitudes (see §1), this section is the starting point for their solution.

A note about flat attractors. Recall that a flat attractor can arise from a two dimensional *IFS* when the fixed points lies along a line and an eigenvector of each map is parallel to this line. However upon encountering a flat attractor, one would proceed to solve it as a one dimensional attractor.

Throughout this section F will be either a similitude or differential contraction locally formative map at the extreme point $\mathbf{p}$. Further assume trajectory maps are parameterized on $0 \leq v \leq 1$.

6.1 *Projected Trajectory Characteristic Functions*

Definition 1. Given a trajectory $\mathbf{t_x}$ through $\mathbf{x}$ we define a one dimensional fractal subset, $D(\mathbf{t_x})$, of the unit interval as follows. If F is a similitude, then $D(\mathbf{t_x})$ is the trace of $\mathbf{t_x}$. If F is a differential contraction then $D(\mathbf{t_x})$ is the projection of the trace of $\mathbf{t_x}$ onto the minor eigenmanifold, that is, letting P_{ℓ_2} be the operator in the plane projecting points onto the minor eigenmanifold $\ell_2 \cup -\ell_2$ parallel to ℓ_1. Put

$$D(\mathbf{t_x}) = P_{\ell_2} A(\mathbf{t_x}).$$

Thus $D(\mathbf{t_x})$, the projected fractal dust, is the subset of the minor eigenmanifold consisting of the v-coordinates of attractor points on the trajectory $\mathbf{t_x}$.

Proposition 1. *The characteristic function* $\chi_{\mathcal{D}(\mathbf{t_x})}$

$$\chi_{\mathcal{D}(\mathbf{t_x})} = \begin{cases} 1, & \text{if } v \in D(\mathbf{t_x}) \\ 0, & \text{otherwise} \end{cases}$$

is asymptotically "multiplicatively periodic" for $\mathbf{x} \in A$ *in some neighborhood of* $\mathbf{p}$, *that is, for some* $0 < \eta \leq 1$ *and some* $\lambda > 0$, $\chi_{\mathcal{D}(\mathbf{t_x})}(v) = \chi_{\mathcal{D}(\mathbf{t_x})}(\lambda v)$ *for all* $0 < v < \eta$.

Proof. Since F is locally formative at $\mathbf{p}$, there exists a neighborhood $\mathcal{N}$ of $\mathbf{p}$ invariant under F or equivalently, under its linear part F in natural coordinates. Let λ_2 be the minor eigenvalue of F. For any $\mathbf{x} = (u_0, v_0) \in \mathcal{N}$ in natural coordinates, we have $F(\mathbf{x}) = (\lambda_1 u_0, \lambda_2 v_0) \in \mathcal{N}$. Hence for v so small that $(\mathbf{t_x}(v), v) \in \mathcal{N}$ then $\lambda_2 v \in D_{\mathbf{t_x}}$ if $v \in D_{\mathbf{t_x}}$. ∎

Definition 2. Let $G(\mathbf{t_x})$ denote the complement of $D(\mathbf{t_x})$ on $(0, 1]$. Since $D(\mathbf{t_x})$ is compact and disconnected, $G(\mathbf{t_x})$ is the countable union of disjoint open intervals, the gaps between the projected fractal dust.

Definition 3. For $\epsilon > 0$, by the *relative ϵ–gaps* of trajectory $\mathbf{t_x}$, we mean the set $G_\epsilon(\mathbf{t_x}) = \{(a, b) \in G(\mathbf{t_x}) : b - a = a\epsilon\}$. Let $\mathcal{G}_\epsilon(\mathbf{t_x}) = \cup_{\eta \geq \epsilon} G_\eta(\mathbf{t_x})$ be the set of all gaps of relative size ϵ or larger.

In the vicinity of a fixed point, gaps are transported by a trajectory map F in the same way as points, cf. Theorem 2.3.2. In particular, there is a dual theory of orbits for gaps just as for points in that a gap along a trajectory is mapped into another gap along the same trajectory by F.

Proposition 2. *For at least one ϵ, G_ϵ is infinite.*

Proof. Let (a, b) be a gap within the neighborhood of invertibility and let ϵ be such that $(a, b) \in G_\epsilon$. If λ is a multiplicative period, then for the gap (a', b') where $a' = \lambda a$ and $b' = \lambda b$,

$$b' - a' = \lambda(b - a) = \lambda a \epsilon = \epsilon a' \tag{6.1}$$

and hence belongs to G_ϵ. By trivial induction, G_ϵ is infinite for ϵ. ∎

Definition 4. Let λ be an asymptotic multiplicative period at $\mathbf{p}$, an *ϵ-gap family started by $g = (a, b)$* is a subset of G_ϵ each member $g_k = (a_k, b_k)$ of which is given by $g_k = \lambda^k g$, i.e. $a_k = \lambda^k a$ and $b_k = \lambda^k b$. Note that for a given ϵ, the terms of G_ϵ need not stem from a single gap family, instead there may be two or even more families represented in G_ϵ. The next Proposition shows, among other things, that there can be at most finitely many families for any given ϵ.

Proposition 3. *The set of ϵ for which G_ϵ is infinite is at most countable and has no limit point other than possibly 0.*

Proof. By the invertibility of powers of locally formative maps, Theorem 2.3.2, there exists a neighborhood of $\mathbf{p}$ inside which all gaps have a preimage. Therefore all starting gaps lie outside some fixed distance $\delta > 0$ from $\mathbf{p}$. From this the result follows. ∎

At this point one can calculate the multiplicative period, or contraction factor, λ given an infinite ϵ–gap family G_ϵ. First order the gaps by size, say $g_1, g_2, \ldots$. Now form a triangular matrix whose ij^{th} entry, for $i > j$, is the ordered pair (g_i, g_j). Traverse the

table, say along lower left to upper right diagonals, and for each entry (g_i, g_j) in the table calculate

$$\lambda = \frac{b_j}{b_i}.$$

We term such a quotient a *candidate multiplicative period* if and only if also $(b_j - a_j)/(b_i - a_i) = \lambda$.

Definition 5. By the spectrum $\Lambda_{\mathbf{x}}$ on the trajectory $\mathbf{t}_{\mathbf{x}}$ we mean the set of all candidate multiplicative periods λ such that λ^k is also a candidate multiplicative period for $k = 2, 3, \ldots$.

Proposition 4. *Let F have minor eigenvalue λ_2 and be locally invariant on the neighborhood $\mathcal{N}$ of $\mathbf{p}$. Then for every $\mathbf{x} \in A \cap \mathcal{N}$, some root, $\sqrt[n]{\lambda_2}$, $n = 1, 2, \ldots$, belongs to $\Lambda_{\mathbf{x}}$. Hence λ_2 also belongs to $\Lambda_{\mathbf{x}}$ for all such $\mathbf{x}$.*

Proof. By the uniqueness Theorem 5.4.1, there can be only one multiplicative period at each $\mathbf{p}$. On the other hand, by "chance," on any one trajectory there can be points of the attractor which give rise to arbitrary roots of periods, cf. the Cantorrows attractor fig. 15. ∎

6.2 *Locally Formative Map Determination by Case*

Let $\mathbf{p}$ be an extreme point of A. By the springbar analysis of §5 applied at $\mathbf{p}$, we form a preliminary determination of the spectral type of the locally formative map F at $\mathbf{p}$, the possibilities are: (a) similitude or false similitude, (b) differential contraction, or (c) GM-1. With the exception of the false similitude case, the results enable the calculation of true trajectories $\mathbf{t}_{\mathbf{x}}$ for each point $\mathbf{x} \in A$. In the false similitude case the trajectories are wrongly assumed to be rays.

In this section we examine the spectral families case by case and show how to make a complete determination of the locally formative map in each case.

This section is organized according to springbar type, rays, exponential trajectories, and harmonic trajectories. From Table 1 of §3, rays occur in the non-rotational similitude, alternating-similitude, and false-similitude cases. Exponential trajectories occur in the exponential and alternating exponential cases. Recall that through positive refinements, we may assume that the alternating cases do not occur.

6.2.1 *Non-Rotational Similitude,* $\lambda_2 = \lambda_1$

In this case the locally formative map F is exactly λI and has only the one unknown parameter λ. Note that every direction is an eigendirection. When F is only locally formative, a given trajectory $\mathbf{t_x}$ either eventually intersects a deleted tile containing $\mathbf{p}$ or eventually only intersects the attractor at $\mathbf{p}$ itself. Therefore by Proposition 6.1.4, every non-empty spectrum will contain the multiplicative period corresponding to the locally formative map F. We summarize this as follows.

Theorem 1. *In the case when* $\lambda_2 = \lambda_1$ *(non-rotational similitude) the parameter* λ *is given by*

$$\lambda = \max \bigcap_{\mathbf{x}} \Lambda_{\mathbf{x}}$$

where $\mathbf{x}$ *is taken over the domain of invariance of* F.

6.2.2 *Exponential,* $\lambda_1 > \lambda_2 > 0$.

As noted in §5.3.2 there are four subcases here depending on the relationship between the eigenmanifolds and the limbs of the convex hull at $\mathbf{p}$: (a) neither coincide with the boundary, (b) ℓ_1 lies on $\partial C(A)$ but ℓ_2 does not, (c) ℓ_2 lies on $\partial C(A)$ but ℓ_1 does not, or (d) both coincide with the boundary (False Similitude case). In the first three cases, either the forward, the backward or both supporting trajectories will be exponential curves.

It follows from Theorem 1 of §5.3.2 that in these three subcases, either the forward, the backward, or both springbar graphs will correctly identify this case and, by Corollary 1 of §5.3.2, allow the calculation trajectory maps. The solution now proceeds similar to that of the Non–Rotational Similitude case treated in §6.2.1 above. We summarize this as follows.

Theorem 2. *In subcases (a), (b), and (c) of the exponential case, the minor eigenvalue* λ_2 *is given by*

$$\lambda_2 = \max \bigcap_{\mathbf{x}} \Lambda_{\mathbf{x}}$$

with the intersection taken over all $\Lambda_{\mathbf{x}}$ *for* $\mathbf{x}$ *in the domain of invariance of* F. *Then the major eigenvalue is given by*

$$\lambda_1 = \lambda_2^{1-\rho}$$

where ρ *is calculated from Corollary 5.3.1.*

6.2.3 *False Similitude, eigendirections coincide with ∂C_A.*

In this case the Springbar Analysis has a similitude signature and therefore the Gap Analysis proceeds as if trajectories are rays. It can be shown by example that (a) both a differential contraction with its eigendirections lying along the limbs of the convex hull and a similitude can both be invariant maps at an extreme point, cf. the Twodcantor attractor fig. 16[1], and (b) that in addition, the similitude can be incomplete in a way we make precise with the concept of residues, cf. the Cantorrows attractor fig. 15.

Definition 1. Let w be an attractor invariant map. We call the set $A - w(A)$ the *residue* of w. If the fixed point $\mathbf{p}$ of w is also a limit point of its residue, then we say the residue is *asymptotic* for w.

In the False Similitude case there are three possibilities: either a similitude and a differential contraction can serve as the solution map at $\mathbf{p}$, or only a differential contraction will serve, no similitude is locally invariant at $\mathbf{p}$, or finally a similitude is invariant at $\mathbf{p}$ but leaves an asymptotic residue.

In the first case our Gap Analysis will find the similitude solution as usual and there will be no asymptotic residue.

In the second case, the Gap Analysis will fail in that the intersection of spectra over all rays will be empty, i.e. no similitude is invariant at $\mathbf{p}$. Consequently it can be inferred that this is a differential contraction with the eigendirections known (namely being the limbs of the convex hull). It remains to determine the eigenvalues, i.e. contraction factors along the eigendirections. Without knowing these values it is not be possible to construct a trajectory map and hence the only spectra available are the two for the eigendirections. On the other hand, these spectra will contain the desired contraction factors. Letting ν_f denote the supremum of Λ_f, we know that the corresponding eigenvalue λ_f is some power of ν_f, i.e. $\lambda_f = \nu_f^{n_f}$ for some integral $n_f > 0$. Similarly for the other contraction factor, $\lambda_b = \nu_b^{n_b}$ for some integral $n_b > 0$ where ν_b is the supremum of Λ_b.

Now solutions for n_f and n_b exist and can be found be trial and error. By a solution we mean a choice for which the resulting differential contraction with eigenvalues λ_f and λ_b yield a locally invariant map w at $\mathbf{p}$ with no asymptotic residue. Of course the smallest such n_f and n_b are the most desirable as they entail the largest corresponding tile at $\mathbf{p}$. The search therefore can proceed along diagonals of a two-way table of the possible values of constant sum, $n_f + n_b =$ constant.

In the third case, similitudes can be invariant at $\mathbf{p}$ but all leave an asymptotic residue. The solution here proceeds just as discussed above.

[1] This example is due to Eugeni Belogay.

Theorem 3. *In the False Similitude case there exist contraction factors λ_f and λ_b such that the locally invariant map w can be constructed.*

6.2.4 *Geometrical Multiplicity One*

By Theorem 5.3.2 the parameter $b = \frac{\gamma}{\lambda \ln \lambda}$ can be calculated from the Springbar analysis. Hence given a point $\mathbf{x} = (u_0, v_0) \in A$, $a = \frac{u_0}{v_0} - b \ln v_0$ can be calculated and hence by (3.8) the trajectory through $\mathbf{x}$ found. As in the other cases, project its trace onto the minor natural coordinate axis. By equation (3.7) this fractal dust is multiplicatively periodic as in the other cases. Now use the gap analysis as before to calculate the spectrum $\Lambda_{\mathbf{x}}$. Then

$$\lambda = \max \bigcap_{\mathbf{x} \in A} \Lambda_{\mathbf{x}}.$$

Now knowing λ, γ is given by

$$\gamma = b\lambda \ln \lambda$$

and the case solved.

Theorem 4. *The GM-1 case can be solved as detailed above.*

7 Encoding Image Tiles

Given an extreme point $\mathbf{p}$, by the techniques of sections 4 and 5, its locally formative map f can be calculated. By testing the action of f on all the points of the attractor it will be seen whether f is globally formative, i.e. a generating map or not. The case that it is not is the subject of this section. Also we treat the encoding of the maps corresponding to *interior* tiles.

We develop in this section a technique for calculating invariant affine maps from primary extreme points to secondary ones which preserve eigendirections and supporting trajectories. Of course any such map can be included in an *IFS* for A. However such a map will not necessarily solve its secondary point for the resulting tile may leave an asymptotic residue. Only if the primary/secondary pair are correctly matched will such a map be a solution for the secondary point (see below). Hence it may be necessary to exhaustively test for correct matches. This will always succeed since there are at most finitely many primary extreme points (and we are assuming A is an *IFS* attractor). Note that decorative maps, unlike formative ones (cf. Theorem 3.2.1), can be rotational similitudes.

7.1 *Encoding Secondary Tiles.*

As in §2, let $\mathbf{p} = w(\mathbf{q})$ where $\mathbf{q}$ is a primary extreme point and w is a decorative globally invariant map for A; our goal in this section is to calculate w. Assume f is the formative map for $\mathbf{q}$, $\mathbf{q} = f(\mathbf{q})$. Then a locally invariant map h is given by $h = wfw^{-1}$. (We invoke

here our rank two assumption on the attractor so that w^{-1} always exists.) Our next theorem is well-known and notes that the spectral characteristics of f and h are identical.

Theorem 1. *Let h, f, and w be as above, and let H, F, and W be their linear parts respectively. Then H and F have identical eigenvalues and $\mathbf{x}$ is an eigenvector of F if and only if $W\mathbf{x}$ is an eigenvector of H.*

By this theorem, the candidate primary extreme points of which $\mathbf{p}$ is the image must have identical spectra to that at $\mathbf{p}$. If more than one primary extreme point qualifies, then the technique below can be applied to each yielding at least one decorative map w as a solution. Hence assume the primary extreme point $\mathbf{q}$ is to be mapped by a decorative map w to the secondary extreme point $\mathbf{p}$.

In addition to the correspondence of eigendirections, there is a correspondence of supporting trajectories.

Theorem 2. *Let $w \in \mathcal{W}$ be the decorative map at $\mathbf{p}$ for $A = A(\mathcal{W})$. If $\mathbf{t}^*$ is a supporting trajectory at the pre-image $\mathbf{q}$ of $\mathbf{p}$, then $w(\mathbf{t}^*)$ is a supporting trajectory at $\mathbf{p}$.*

Proof. Obviously $w(\mathbf{t}^*)$ has a complete trace at $\mathbf{p}$. Since affine maps preserve order, no image of a complete trace at $\mathbf{q}$ lies beyond that of $w(\mathbf{t}^*)$. It follows that if there is a complete trace at $\mathbf{p}$ beyond that of $w(\mathbf{t}^*)$, it must belong to different tile than $\mathbf{p}$ but have $\mathbf{p}$ as a limit point. But this is impossible since tiles are closed and disjoint. ∎

Hence supporting trajectories go into supporting trajectories under decorative maps. Nevertheless the different spectral cases of the formative maps require different treatments.

7.1.1 *Differential Contraction Case*

In all three spectral cases we seek the 6 affine parameters defining a decorative map w. We will use the condition that the primary point $\mathbf{q}$ must map to the secondary extreme point $\mathbf{p}$ to solve for the translational part of w. Hence the problem is reduced to finding the 4 elements of the linear part W.

In the differential contraction case we have distinct eigenvalues and eigenvectors to work with, and since by Theorem 1 these must correspond between the primary and its secondary, the problem is reduced to two parameters. This may be seen as follows. Using the eigenvectors in both the domain and range of w as bases, its linear part diagonalizes to a matrix of the form

$$\Lambda = \begin{pmatrix} g & 0 \\ 0 & h \end{pmatrix}$$

where the parameters g and h stem from the as yet unknown contractions along the eigendirections.

Additionally from Theorem 2 we know that the supporting trajectories must correspond. Let $u = u_0\lambda_1^t$, $v = v_0\lambda_2^t$ and $r = r_0\lambda_1^\tau$, $s = s_0\lambda_2^\tau$ be the forward supporting

trajectories at the primary and secondary extreme points respectively. In these equations t and τ are the independent variables, u, v, r, and s are the natural coordinate dependent variables and all other parameters are known. Mapping the primary trajectory by Λ gives $(\, r \quad s \,)^T = \Lambda \, (\, u \quad v \,)^T$ or

$$r_0 \lambda_1^{\tau} = g u_0 \lambda_1^{t} \qquad \text{and} \qquad s_0 \lambda_2^{\tau} = h v_0 \lambda_2^{t} \tag{7.1}$$

which holds in the sense that for each t there exists a τ for which both equations hold. In particular this is true for $t = 0$ with some corresponding value τ_0; that is

$$r_0 \lambda_1^{\tau_0} = u_0 g \qquad \text{and} \qquad s_0 \lambda_2^{\tau_0} = v_0 h.$$

A similar calculation can be made for the backward supporting trajectory; however the resulting equation is not independent. Thus we are left with 3 unknowns but only two equations. We show how to calculate one of g or h directly next. It follows that the other may be found from (7.1) and the required map solved.

Given $g > 0$ the decorative map, say w_g, will be completely determined. We define $H(g)$ to be the one-sided Hausdorff set distance from $w_g(A)$ to A, that is

$$H(g) = \sup_{\mathbf{b} \in w_g(A)} \inf_{\mathbf{a} \in A} \|\mathbf{a} - \mathbf{b}\|_2$$

see (Shonkwiler, 1989). Evidently $H(g)$ is zero if and only if $w_g(A) \subset A$, that is if and only if w_g is invariant for that particular choice of g. Denote the set of such values by G,

$$G = H^{-1}(0). \tag{7.2}$$

Since w_g is invertible, the set of such points g has no limit point other than the origin.

It remains to satisfy the residue property. If the primary and secondary are correctly matched, then one or more values of $g \in G$ will not have an asymptotic residue. To select out these values, we form the one-sided Hausdorff distance $\mathcal{H}_g$ from the $w_g^{-1}(A \cap w_g(C_A))$ to A, where as usual C_A is the convex hull of A,

$$\mathcal{H}_g = \sup_{\mathbf{b} \in w_g^{-1}(A \cap w_g(C_A))} \inf_{\mathbf{a} \in A} \|\mathbf{a} - \mathbf{b}\|_2.$$

As above, this is zero if and only if $w_g^{-1}(A \cap w_g(C_A)) \subset A$, implying w_g leaves no asymptotic residue.

7.1.2 *GM-1, Harmonic Case*

This goes just as above, using natural coordinates reduces the problem to solving for the diagonal matrix Λ. Matching harmonic supporting trajectories between primary and secondary reduces the problem to finding one of g or h directly. And one of these may be determined by assuring both $w_g(A) \subset A$ and $w_g^{-1}(A \cap w_g(C_A)) \subset A$.

7.1.3 *Similitude Case*

Unfortunately here all rays are eigendirections and consequently there will be no equation stemming from their correspondence. However by using supporting trajectories as the basis for natural coordinates, as we have (cf. §3.3), reduces the problem to solving the diagonal matrix Λ as before.

Before showing how to find suitable values for g and h, note that it will not be known in advance to which secondary supporting trajectory, forward or backward, the forward supporting primary trajectory will map. Hence the following procedure might have to be applied to both possibilities.

As above, to each pair of values (g, h) there will correspond a decorative map, $w_{(g,h)}$, which preserves supporting trajectories. Define again the one-sided Hausdorff distance, $H(g, h)$, from $w_{(g,h)}(A)$ to A, that is

$$H(g,h) = \sup_{\mathbf{b} \in w_{(g,h)}(A)} \inf_{\mathbf{a} \in A} \|\mathbf{a} - \mathbf{b}\|_2$$

Evidently $H(g, h)$ is zero if and only if $w_{(g,h)}(A) \subset A$, that is if and only if $w_{(g,h)}$ is invariant for that particular choice of g and h. Since $w_{(g,h)}$ is invertible, the set of such pairs has no limit point other than the origin. As above, let $G = H^{-1}(0)$. Again assuming there is a solution for the chosen primary and secondary, the set of all pairs $(g, h) \in G$ for which the one-sided Hausdorff distance $\mathcal{H}$ from $w_{(g,h)}^{-1}(A \cap w_{(g,h)}(C_A))$ to A is zero is non-empty and any such pair constitutes a solution. The pair with largest product, gh, is the optimal pair to use as it has the largest Jacobian.

Theorem 3. *Using the procedure described above of matching primary and secondary extreme points, corresponding eigendirections, corresponding forward or backward supporting trajectories and choosing the parameter g (or the parameters g and h) so that both one-sided Hausdorff distances H and $\mathcal{H}$ are zero calculates a decorative map w which tiles the secondary extreme point.*

7.1.4 *False Similitude Case*

Of course if a False Similitude primary extreme point is mapped by some decorative map of an *IFS* to a secondary extreme point, then that secondary extreme point will react to the springbar and gap tests just as primary does. And of course its locally formative solution follows in the same way. Therefore, as above, the match of spectral signatures identifies corresponding extreme points.

Solving the secondary extreme point proceeds exactly as in the Similitude case, matching supporting trajectories, and in the final stage, insuring the map be invariant and leaving no asymptotic residue. Thus there are no special problems here.

7.2 *Encoding Interior Tiles*

7.2.1 *One Dimensional Solution.*

The main problem is finding the interior points at which to apply the gap analysis. We will use the gaps themselves for this.[1]

Theorem 1. *Let x be an end point of any gap. Then x is the fixed point of some invertible locally formative map.*

Proof. If C is the convex hull of A, then

$$A = \bigcap_{k\to\infty} \bigcup_{i_1,\ldots,i_k} w_{i_1}\ldots w_{i_k}(C)$$

and hence the gaps are given by

$$\bigcup_{k\to\infty} \bigcap_{i_1,\ldots,i_k} [w_{i_1}\ldots w_{i_k}(C)]^c$$

in which the intersections are over open intervals. Each resulting intersection is a gap,

$$g = \bigcap_{i_1,\ldots,i_k} [w_{i_1}\ldots w_{i_k}(C)]^c$$

any endpoint **x** of which is an endpoint of one of the sets $w_{i_1}\ldots w_{i_k}(C)$. But this composition is the required locally formative map of the theorem – or possibly with further refinement to yield a smaller but strongly disjoint tile. ∎

It has already been noted that the gaps in an attractor (with at least two generating *IFS* maps) are countable and may be well ordered by length. Since the sets $w_i(A)$, are disjoint compact sets for some *IFS* $\mathcal{W}$ for A, it follows that the gaps flanking the endpoints

[1] The authors thank George Donovan for his discussion of this point leading to the idea.

of the convex hull C_{w_i} of $w_i(A)$ have a minimum length, $\delta > 0$. Hence candidate points for starting the gap analysis to solve interior tiles are included in the set of end points of the initial part of the gap list down to gaps the size δ or larger, a finite set, cf. Theorem 2.3.2.

At any point in the solution process, the points of A can be classified into two sets U and R, unresolved and resolved respectively. One might say the points in R are "colored". A point r of the latter are images $r = w(a)$ of some point $a \in A$ under some map w determined by the solution process so far. The solution process is done when all points of A are colored. Since the solving process always finds the largest map (in terms of eigenvalue) invariant for the attractor at every step, the attractor will be solved by the foregoing techniques when the process has been applied to the candidate end points as described above corresponding to that minimal *IFS*.

Of course the largest gap will flank tiles in any *IFS*. However subsequent gaps in the well-ordered list need not. The gap analysis applied to one of these will calculate a subtile that may eventually be discarded.

Theorem 2. *Given a disjoint one-dimensional attractor A, the gap solution procedure as detailed above constructs an IFS in finitely many steps whose attractor is A.*

7.2.2 *Two Dimensional Solution.*

Proposition 1. *The affine image of a convex polygon is a convex polygon.*

Proof. This is an easy observation from the fact that an affine map takes half-spaces into half-spaces. ∎

Proposition 2. *The finite disjoint union of convex polygons is polyhulled.*

Proof. This is an elementary observation.

Definition 1. For a given PHD attractor A let Ω denote the collection of all pairs (γ, ϵ) where γ is a simple closed curve lying in A^c and $\epsilon = \text{dist}(\gamma, A)$.

The relation $(\gamma_1, \epsilon_1) \equiv (\gamma_2, \epsilon_2)$ if and only if γ_1 can be homotoped to γ_2 within A^c is an equivalence relation on Ω and hence divides it into equivalence classes. We exclude from further consideration the null-homotopic curves. For each such equivalence class, Γ, let $\epsilon_\Gamma = \max\{\epsilon : (\gamma, \epsilon) \in \Gamma\}$. The set of maximum epsilons is countable and of course is naturally ordered large to small. In case of ties, and there can be only finitely many ties, any order will suffice.

Theorem 3. *Let $\mathcal{W}$ be an IFS for A. The portion of A inside any closed curve as above is the union of tiles of some refinement of $\mathcal{W}$.*

Proof. As $k \to \infty$ the diameter of the tiles of the power refinement $\mathcal{W}^k$ tend to zero. By Theorem 2.2.1 there is a minimum distance $\delta > 0$ separating tiles of the disjoint *IFS* $\mathcal{W}$. Thus for k sufficiently large so that tile diameter is less than δ it will be that only complete tiles of $\mathcal{W}^k$ will lie inside a given closed curve. ∎

Corollary 1. *The extreme points of the portion of A inside any closed curve as in the Theorem are images of extreme points of A under some affine map.*

Proof. By Propositions 1 and 2, the convex hull of such a restriction sub-attractor is polyhulled and by the Theorem, its extreme points belong to affine images of tiles of A. But the extreme point of an affine image of a tile, must be the image of an extreme point of the tile. ∎

Now solve interior tiles as follows. If the solution of all extreme points leaves no residue, then we are done. Otherwise for each equivalence class Γ starting with the largest max epsilon, solve all the extreme points of the Γ-deleted attractor, namely $A \cap \Gamma^0$ the interior of any $\gamma \in \Gamma$. The solution for the extreme points of this deleted attractor will go just as secondary extreme points. In finitely many steps, proceeding from large to small max epsilon, the residue will become empty and the attractor solved.

8 Limits of PHD Attractors

Theorem 1. *Let $\mathcal{W}_n = \{w_1^{(n)}, \ldots, w_r^{(n)}\}_1^\infty$ be a sequence of iterated function systems each having r affine maps. By stringing out the $6r$ parameters of these maps, each $\mathcal{W}_n$ may be identified with a point,v_n, in $6r$ dimensional Euclidean space. Suppose $v_n \to v$ as $n \to \infty$ and $\mathcal{W}$ is the IFS identified with v. Then the sequence of contraction factors s_n of the $\mathcal{W}_n$ converges to s, the contraction factor of $\mathcal{W}$. Further, if $s < 1$, then the sequence of attractors A_n of the $\mathcal{W}_n$ converges to the attractor A of $\mathcal{W}$.*

Proof. See [Barnsley,113]. ∎

Theorem 2. *Let $\{A_i\}$ be a sequence of PHD attractors each having n-map IFS's $\mathcal{W}_i = \{w_{i1}, w_{i2}, \ldots, w_{in}\}$ whose tiles $\{w_{ik}\}_{i=1}^\infty$ converge in the Hausdorff metric on compact subset of X for $k = 1, \ldots, n$. Then:*

1 the sequence $\{A_i\}$ converges to a polyhulled attractor A,

2 if the sequence of geometrical multiplicities of the globally formative maps, w_{ij}, converges, then the limits $w_i = \lim_k w_{ik}$ exist and A is the attractor of the IFS $\mathcal{W} = \{w_1, w_2, \ldots, w_n\}$.

Proof. Let $\{E_{ij}\}_{j=1}^{j_i}$, denote the extreme points of A_i, for $i = 1, 2, \ldots$. By using a standard diagonalization argument if necessary we may assume without loss of generality that j_i is constant for i sufficiently large, say equal to J, and the points E_{ij} converge to E_j,

$j = 1, \ldots, J$, say, as $i \to \infty$. By considering convex combinations (which are linear) and noting continuity of this representation, we see that the $\{E_j\}_1^J$ contain the extreme points of the limit set $A = \lim_i A_i$.

We can show, case by case, that the spectral properties of each extreme point E_{ij} converges as a function of i. For example suppose for each i the spectral type is differential contraction and the limiting extreme point is also. Assume the limiting spectrum is not the limit of the sequential spectra. Then there exists a cone of half-angle δ and an i arbitrarily large such that the asymptote ℓ_i of A_i lies outside the δ-cone. Now since the supporting trajectory $\mathbf{t}_i^*$ of A_i converges exponentially to ℓ_i while the cone converges linearly to ℓ_i, there is a ball of radius r, B_r, such that $\mathbf{t}^*$ lies outside the cone but inside B_r. This shows that A_i exceeds in Hausdorff metric the distance $\delta r/2$, contradiction. ∎

Remark. *This result allows a nice application of this work to fractal functions.*

Examples

Let

$$W_\epsilon = \begin{pmatrix} \frac{1}{2} + \epsilon & 0 \\ 0 & \frac{1}{2} + \epsilon \end{pmatrix}.$$

The 3-map *IFS*

$$w_1(\epsilon) = W_\epsilon, \quad w_2(\epsilon) = W_\epsilon + \begin{pmatrix} \frac{1}{2} + \epsilon \\ 0 \end{pmatrix}, \quad w_3(\epsilon) = \mathcal{W}_\epsilon + \begin{pmatrix} \frac{1}{4} + \frac{\epsilon}{2} \\ \frac{1}{2} + \epsilon \end{pmatrix}.$$

The 4-map *IFS* consisting of $w_1(\epsilon), w_2(\epsilon)$ from above and

$$w_a(\epsilon) = W_\epsilon + \begin{pmatrix} 0 \\ \frac{1}{2} + \epsilon \end{pmatrix} \quad w_b(\epsilon) = W_\epsilon + \begin{pmatrix} \frac{1}{2} + \epsilon \\ \frac{1}{2} + \epsilon \end{pmatrix}.$$

		symmetric part				fixed point		
name	figure	a	b	c	rotation	x	y	remarks
shrub	7	.6	0	.667	0	.5	1	not disjoint,
		.333	0	.5	-30	.68	.53	but all
		.333	0	.5	30	.22	.8	tiles
		.6	0	.667	0	.5	0	exposed
Black	8	.85	0.0002	.84	-2.7	.72	.82	not polyhulled
Spleenwort		.3	0	.3	55	.46	.124	
fern		.3	0	.36	-55	.52	.0.06	
dragon	9	.707	0	.707	-45	.625	.625	just touching
		.707	0	.707	-45	.375	.375	attractor
dragontails	10	.5	0	.5	90	.4	.2	no primary
		.5	0	.5	90	.8	.4	point
		.5	0	-0.5	90	.333	.667	
3–map fern	11	-0.9	0	.9	0	.5	.98	alternating
		.3	0	.36	-55	.52	0.06	similitude
		0.0002	0	.16	0	.5	0	
exhar	12	.335	-.112	.783	-26.6	.5	1	exponential
		.333	0	.333	0	1	.5	and
		.333	0	.333	0	0	.5	harmonic
		.333	0	.667	-15	.5	.25	trajectories
gasketflip	13	.5	0	.5	0	0	0	multiple
		.5	0	.5	0	0	1	extreme points
		-.5	0	.5	0	.667	.5	per tile
gasketmod	14	.5	0	.5	0	.5	1	not
		.5	0	.5	0	0	0	strongly
		.5	0	.5	0	1	0	disjoint
		-.125	0	-.125	0	.5	.639	
Cantorrows	15	.333	0	.111	0	0	0	similitude
		.333	0	0	0	0	1	invariant
		.333	0	0	0	1	1	but
		.333	0	0	0	1	0	residue
		.333	0	0	0	0	.333	asymptotic
Twodcantor	16	.333	0	.333	0	0	0	differential
		.333	0	.333	0	0	1	contraction
		.333	0	.333	0	1	0	or similitude
		.333	0	.333	0	1	1	solve

Table 1

References

[1] S. Abenda and G. Turchetti, Inverse problems for fractal sets on the real line via the moment method. *Il Nuovo Cimento*, Vol. 104 B, No. 2, 213–227, (1989)

[2] [BD85] Barnsley, M. Demko, S., "Iterated Function Systems and the Global Construction of Fractals", *Proc. R. Soc. Lond. A* **399** (1985), 243-275.

[3] Barnsley, M.F., *Fractals Everywhere*, Academic Press, NY, (1988)

[4] M.F. Barnsley, V. Ervin, D. Hardin, and J. Lancaster, *Solution of the Inverse Problem for Fractals and Other Sets*, Proc. Nat. Acad. Sci. **83**, 1975-1977 (1985)

[5] M. Barnsley, and A. Sloan, *Image Compression by Simulated Thermal Annealing*, DARPA proposal, (1985)

[6] Berger, M., "Random Affine Iterated Function Systems: Mixing and Encoding", *Difusion Processes and Related Problems in Analysis, Vol. II: Stochastic Flows*, Pinsky, M. and Wihstutz, V., eds, Birkhäuser, Boston (1991)

[7] Bessis, D and Demko, S., "Stable Recovery of Fractal Measures by Polynomial Sampling", *preprint, School of Math., Georgia Institute of Technology*, (1990)

[8] C.A. Cabrelli, U.M. Molter and E.R.Vrscay, "Moment Matching for the approximation of measures using Iterated Function Systems," (preprint, 1992)

[9] C.A. Cabrelli, B. Forte, U.M. Molter and E.R. Vrscay, "Iterated fuzzy set systems: a new approach to the inverse problem for fractals and other sets," to appear in J. Math. Anal. Appl. in August, 1992.

[10] Demko, S., "IFS Methods for the Inverse Fractal Problem", sl preprint, School of Math. Georgia Institute of Technology, (1990a)

[11] Demko, S., "Approximation of Measures by Fractal Generation Techniques", *preprint, School of Math., Georgia Institute of Technology, Atlanta, 30332*, (1990b)

[12] Falconer, K.J., *The geometry of fractal sets*, Cambridge University Press, (1985)

[13] Hutchinson, J., *Fractals and selfsimilarity*, Indians Univ. J. Math., **30**, 713-747 (1981)

[14] C. Handy and G. Mantica, *Inverse Problems in Fractal Construction: Moment Method Solution*, Physica D (to appear)

[15] Mantica, G., and Sloan, A., *Chaotic optimization and the construction of fractals: solution of an inverse problem*, Complex Systems, **3**, 37-62 (1989)

[16] Sz.-Nagy, B., *Extensions of Linear Transformations in Hilbert Space which Extend Beyond this Space*, Frederick Ungar, New York, (1960)

[17] "Dimensions Associated with Recurrent Self-Similar Sets," J. of Cambridge Philo. Soc. (to appear) (with A. Deliu, J. Geronimo, and D. Hardin).

[18] Diaconis, P. M. and Shahshahani, M., "Products of Random Matrices and Computer Image Generation," *Contempory Math.*, 50:173–182 (1986)

[19] Mandelbrot, B., *The Fractal Geometry of Nature*, W. H. Freeman and Co., San Francisco, (1982)

[20] Shonkwiler, R., "An Image Algorithm for Computing the Hausdorff Distance Efficiently in Linear Time", *Inf. Proc. Letters* **30** (1989), 87-89.

[21] Strichartz, R., "A Fractal Radon Inversion Problem", *preprint, Math. Dept., White Hall, Cornell University, Ithaca, N.Y. 14853*, (1993)

[22] Vrscay, R., *Moment and collage methods for the inverse problem of fractal construction with iterated function systems*, Fractal 90 Conference, Lisbon, June 6-8, 1990.

[23] E.R. Vrscay and C.J. Roehrig, "Iterated function systems and the inverse problem of fractal construction using moments, "Computers and Mathematics, E. Kaltofen and S.M. Watt, Editors (Springer Verlag, 1989), pp. 250-259.

[24] E.R.Vrscay, "Iterated function systems: theory, applications and the inverse problem," in "Fractal Geometry and Analysis", Proceedings of the NATO Advanced Study Institute, Montreal, Canada, July 3-21, 1989, J. Belair and S. Dubuc, Editors; pp 405-468s (Kluwer, Dordrecht, the Netherlands, 1991).

[25] E.R.Vrscay, "Moment and collage methods for the inverse problem of fractal construction with Iterated Function Systems," in "Fractals in the Fundamental and Applied Sciences, H.-O. Peitgen, J.M. Henriques and L.F. Penedo, Editors (Elsevier, 1991).

fig. 7

fig. 8

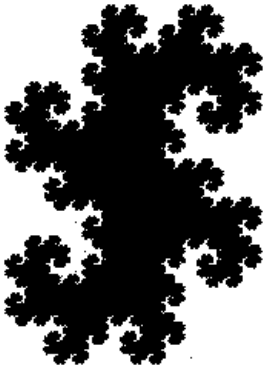

fig. 9

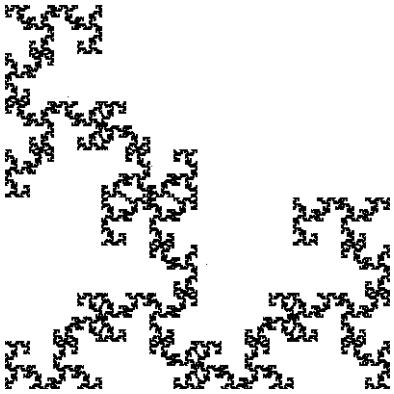

fig. 10

fig. 11

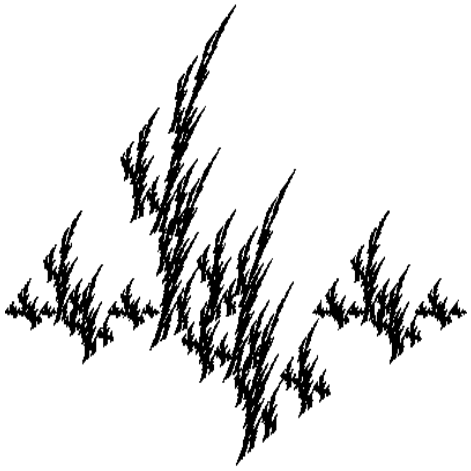

fig. 12

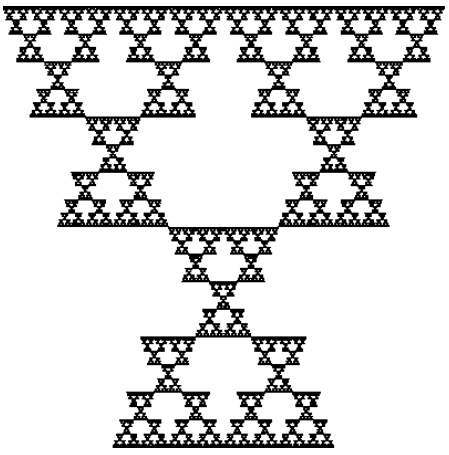

fig. 13

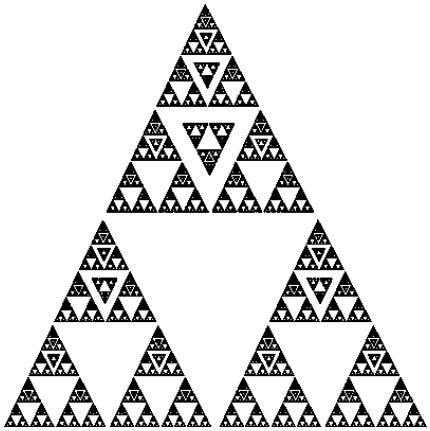

fig. 14

fig. 15

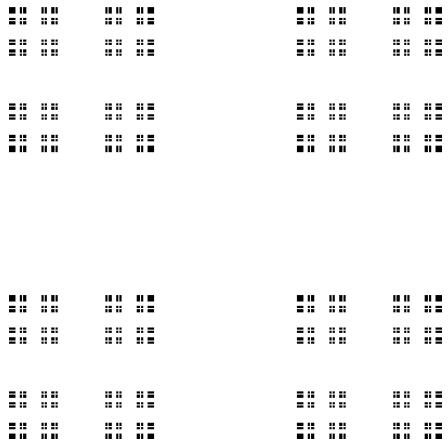

fig. 16